

AD-A115 080

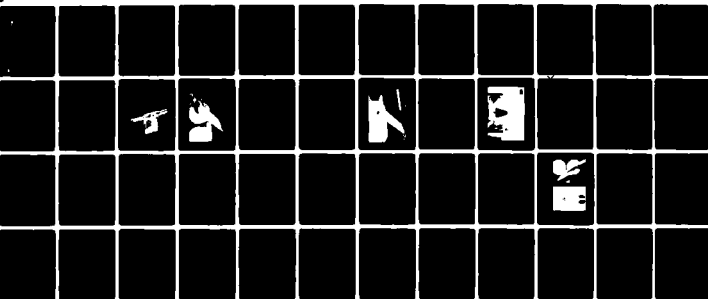
CALSPAN FIELD SERVICES INC ARNOLD AFS TN AEDC DIV F/G 22/2  
NASA/ROCKWELL INTERNATIONAL SPACE SHUTTLE ORBITER ABORT HEATING--ETC(U)  
NOV 81 L A TICATCH, K W MUTT

UNCLASSIFIED

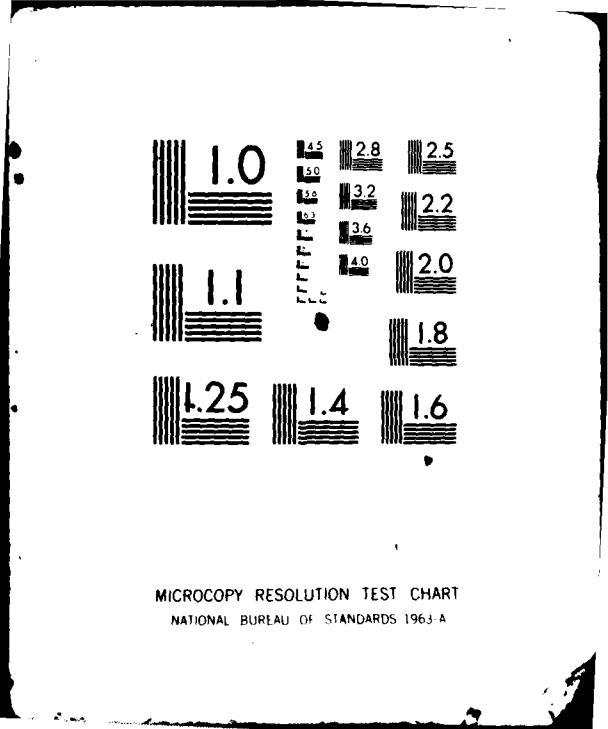
AEDC-TSR-81-V36

NL

1001  
A-115-080



END  
DATE  
FILMED  
7-82  
DTIC



AEDC-TSR-81-V36

2

AD A115020



NASA/ROCKWELL INTERNATIONAL SPACE SHUTTLE  
ORBITER ABORT HEATING TEST (OH-111)

L. A. Ticatch and K. W. Nutt  
Calspan Field Services, Inc.

November 1981

Final Report for Period September 25-30, 1981

Approved for public release; distribution unlimited.

DTIC  
ELECTE  
JUN 02 1982  
S D E

ARNOLD ENGINEERING DEVELOPMENT CENTER  
ARNOLD AIR FORCE STATION, TENNESSEE  
AIR FORCE SYSTEMS COMMAND  
UNITED STATES AIR FORCE

82 06 01 177

#### NOTICES

When U. S. Government drawings, specifications, or other data are used for any purpose other than a definitely related Government procurement operation, the Government thereby incurs no responsibility nor any obligation whatsoever, and the fact that the Government may have formulated, furnished, or in any way supplied the said drawings, specifications, or other data, is not to be regarded by implication or otherwise, or in any manner licensing the holder or any other person or corporation, or conveying any rights or permission to manufacture, use, or sell any patented invention that may in any way be related thereto.

References to named commercial products in this report are not to be considered in any sense as an endorsement of the product by the United States Air Force or the Government.

This report has been reviewed by the Office of Public Affairs (PA) and is releasable to the National Technical Information Service (NTIS). At NTIS, it will be available to the general public, including foreign nations.

#### APPROVAL STATEMENT

This report has been reviewed and approved.

*J. T. Best*

J. T. BEST  
Aeronautical Systems Branch  
Deputy for Operations

Approved for publication:

FOR THE COMMANDER

*John M. Rampy*  
JOHN M. RAMPY, Director  
Aerospace Flight Dynamics Test  
Deputy for Operations

# UNCLASSIFIED

SECURITY CLASSIFICATION OF THIS PAGE (When Data Entered)

REPORT DOCUMENTATION PAGE		READ INSTRUCTIONS BEFORE COMPLETING FORM
1. REPORT NUMBER AEDC-TSR-81-V36	2. GOVT ACCESSION NO. A0-A115020	3. RECIPIENT'S CATALOG NUMBER
4. TITLE (and Subtitle) NASA/ROCKWELL INTERNATIONAL SPACE SHUTTLE ORBITER ABORT HEATING TEST (OH-111)		5. TYPE OF REPORT & PERIOD COVERED Final Report September 25-30, 1981
7. AUTHOR(s) L. A. Ticatch and K. W. Nutt, Calspan Field Services, Inc./AEDC Division		6. PERFORMING ORG. REPORT NUMBER
9. PERFORMING ORGANIZATION NAME AND ADDRESS Arnold Engineering Development Center Air Force Systems Command Arnold Air Force Station, TN 37389		8. CONTRACT OR GRANT NUMBER(s)
11. CONTROLLING OFFICE NAME AND ADDRESS Johnson Space Center (NASA-JSC(ES3)) Houston, Texas 77058		10. PROGRAM ELEMENT, PROJECT, TASK AREA & WORK UNIT NUMBERS Program Element 921E01 Control No. 9E01
14. MONITORING AGENCY NAME & ADDRESS (if different from Controlling Office)		12. REPORT DATE November 1981
		13. NUMBER OF PAGES 53
		15. SECURITY CLASS. (of this report) UNCLASSIFIED
		15a. DECLASSIFICATION/DOWNGRADING SCHEDULE N/A
16. DISTRIBUTION STATEMENT (of this Report)  Approved for public release; distribution unlimited.		
17. DISTRIBUTION STATEMENT (of the abstract entered in Block 20, if different from Report)		
18. SUPPLEMENTARY NOTES  Available in Defense Technical Information Center (DTIC).		
19. KEY WORDS (Continue on reverse side if necessary and identify by block number) heat transfer thin skin space shuttle orbiter hypersonic testing		
20. ABSTRACT (Continue on reverse side if necessary and identify by block number) Thin-skin thermocouple heat transfer tests were conducted on two 0.0175 scale and one 0.04 scale models of the Space Shuttle orbiter at attitudes that would be encountered in a transatlantic abort maneuver. The model angles of attack ranged from 40 to 55 degrees with yaw angle varying from -2 to 2 degrees. Data were obtained at Mach 8 in the AEDC-VKF Hypersonic Wind Tunnel B at free-stream Reynolds numbers ranging from $0.5 \times 10^6$ to $1.5 \times 10^6$ per foot.		

DD FORM 1 JAN 73 1473

EDITION OF 1 NOV 65 IS OBSOLETE

## UNCLASSIFIED

SECURITY CLASSIFICATION OF THIS PAGE (When Data Entered)

## CONTENTS

	<u>Page</u>
NOMENCLATURE . . . . .	3
1.0 INTRODUCTION . . . . .	6
2.0 APPARATUS	
2.1 Test Facility . . . . .	6
2.2 Test Articles . . . . .	7
2.3 Test Instrumentation	
2.3.1 Test Conditions . . . . .	7
2.3.2 Test Data . . . . .	8
3.0 TEST DESCRIPTION	
3.1 Test Conditions . . . . .	8
3.2 Test Procedure	
3.2.1 General . . . . .	8
3.2.2 Thin-Skin Thermocouple . . . . .	9
3.2.3 Oil-Flow . . . . .	9
3.3 Data Reduction	
3.3.1 Thin-Skin Thermocouple Data . . . . .	9
3.4 Uncertainty of Measurements . . . . .	11
4.0 DATA PACKAGE PRESENTATION . . . . .	12
REFERENCES . . . . .	12

## APPENDIXES

### I. ILLUSTRATIONS

#### Figure

1. Tunnel B. . . . .	14
2. Installation Photograph of 60-0 Model . . . . .	15
3. 60-0 Model Installation . . . . .	16
4. Basic Dimensions and Coordinate System for the 0.0175 Scale Orbiter Models . . . . .	17
5. Installation Photograph of 56-0 Model . . . . .	18
6. 56-0 Model Installation . . . . .	19
7. Installation Photograph of 83-0 Model . . . . .	20
8. 83-0 Model Installation . . . . .	21
9. Basic Dimensions and Coordinate System for the 83-0 Model	22
10. Thermocouple Locations on 60-0 Model . . . . .	23
11. Thermocouple Locations on 56-0 Model . . . . .	29
12. Thermocouple Locations on 83-0 Model . . . . .	30
13. Thin-Skin Thermocouple Plotted Data . . . . .	34
14. Oil-Flow Photographs on 60-0 Model (Run 262) . . . . .	35

### II. TABLES

#### Table

1. Data Transmittal Summary . . . . .	37
2. Estimated Uncertainties . . . . .	38
3. 60-0 Model Thermocouple Coordinates . . . . .	40
4. 56-0 Model Thermocouple Coordinates . . . . .	43

	<u>Page</u>
5. 83-0 Model Thermocouple Coordinates . . . . .	44
6. Test Data Summary . . . . .	47
7. Photographic Summary . . . . .	50
III REFERENCE HEAT-TRANSFER COEFFICIENTS . . . . .	51
IV SAMPLE TABULATED DATA	
1. Thin-Skin Thermocouple Tabulated Data. . . . .	53

Accession For	
NTIS GRA&I	<input checked="" type="checkbox"/>
DTIC TAB	<input type="checkbox"/>
Unannounced	<input type="checkbox"/>
Justification	
By	
Distribution/	
Availability Codes	
Dist	Avail and/or Special
A	



# NOMENCLATURE

ALPI	Indicated pitch angle, deg
ALPHA	Angle of attack, deg
ALPPB	Prebend angle, deg
b	Model skin thickness, in.
B	Wing span, in. (see Fig. 4)
BV	Height of model vertical tail, in. (see Fig. 4)
c	Model material specific heat, Btu/lbm-°R
C	Local chord of wing or vertical tail, in. (see Fig. 4)
DELTA E	Elevon deflection angle, deg
DELTA S B	Speed brake deflection angle, deg
DELTA B F	Body flap deflection angle, deg
DTW/DT	Derivative of the model wall temperature with respect to time, °R/sec
H(REF)	Reference heat transfer coefficient (see Appendix III)
H(TR), H(TT) H(0.9TT), H(0.85TT)	Heat-transfer coefficient based on recovery temperature, TR (TR = TT, 0.9TT, or 0.85TT assumed for these data), $QDOT/(TR-TW)$ , Btu/ft <sup>2</sup> -sec-°R
L	Reference length, in. (see Fig. 4)
M, MACH NO.	Free-stream Mach number
MU	Dynamic viscosity based on free-stream temperature, lbf-sec/ft <sup>2</sup>



MUTT	Dynamic viscosity based on TT, $\text{lbf-sec/ft}^2$
P	Free-stream static pressure, psia
PT	Tunnel stilling chamber pressure, psia
PT2	Stagnation pressure downstream of a normal shock, psia
PHI	Radial angle location of thermocouple in model coordinates, deg (see Figs. 4 and 9)
PHII	Indicated roll angle, deg
Q	Free-stream dynamic pressure, psia
QDOT	Heat-transfer rate, $\text{Btu/ft}^2\text{-sec}$
RE	Free-stream unit Reynolds number, $\text{ft}^{-1}$
RHO	Free-stream density, $\text{lbm/ft}^3$
RN	Reference nose radius, (0.0175 ft or 0.04 ft, determined by model scale)
RUN	Data set identification number
STFR	Stanton number based on reference conditions (see Appendix III)
T	Free-stream static temperature, °R
TC NO	Thermocouple identification number
TIME	Elapsed time from lift-off, sec
TR	Assumed recovery temperature, °R
TT	Tunnel stilling chamber temperature, °R
TW	Model surface temperature, °R

V	Free-stream velocity, ft/sec
X	Model scale axial coordinate from model nose or leading edge of wing or vertical tail (see Fig. 4 and 9) in.
X0	Full scale axial coordinate from a point 235 in. ahead of the orbiter nose (see Fig. 9), in.
Y	Model scale lateral coordinate (see Fig. 4), in.
YAW	Yaw angle of model, deg
Y0	Full scale lateral coordinate, in.
Z	Model scale vertical coordinate (see Fig. 4), in.
Z0	Full scale vertical coordinate, in.
$\rho$	Model material density, lbm/ft <sup>3</sup>

## 1.0 INTRODUCTION

The work reported herein was performed by the Arnold Engineering Development Center (AEDC), Air Force Systems Command (AFSC), under Program Element 921E01, Control Number 9E01, at the request of the Johnson Space Center (NASA-JSC(ES3)), Houston, Texas. The NASA-JSC (ES3) program manager was Mrs. Dorothy B. Lee and the Rockwell International project engineers were Mr. C. L. Berthold and Mr. J. Gee. The results were obtained by Calspan Field Services, Inc./AEDC Division, operating contractor for the Aerospace Flight Dynamics testing effort at the AEDC, AFSC, Arnold Air Force Station, Tennessee. The tests were performed in the von Karman Gas Dynamics Facility (VKF), under AEDC Project No. C628VB.

The test was performed in the 50-in.-diam Hypersonic Wind Tunnel (B) at the von Karman Gas Dynamics Facility (VKF) during the period September 25, 1981 to September 30, 1981. Data were recorded at Mach number 8 for nominal Reynolds numbers ranging from  $0.5 \times 10^6$  to  $1.5 \times 10^6$  per foot. The nominal model angles of attack ranged from 40 to 55 degrees with model yaw angles varying from -2 to 2 degrees. All thin-skin thermocouple data were obtained from three space shuttle orbiter models designated 56-0, 60-0, and 83-0.

The test had a NASA/Rockwell designation of OH-111. The test objective was to obtain thin-skin heat transfer data on the space shuttle orbiter model at attitudes that would be encountered in a transatlantic abort maneuver.

A summary of the test data transmitted is shown in Table 1. Inquiries to obtain copies of the test data should be directed to NASA-JSC (ES3), Houston, Texas 77058. A microfilm record has been retained in the VKF at AEDC.

## 2.0 APPARATUS

### 2.1 TEST FACILITY

Tunnel B (Fig. 1), is a closed circuit hypersonic wind tunnel with a 50-in. diam test section. Two axisymmetric contoured nozzles are available to provide Mach numbers of 6 and 8 and the tunnel may be operated continuously over a range of pressure levels from 20 to 300 psia at Mach number 6, and 50 to 900 psia at Mach number 8, with air supplied by the VKF main compressor plant. Stagnation temperatures sufficient to avoid air liquefaction in the test section (up to 1350°R) are obtained through the use of a natural gas fired combustion heater. The entire tunnel (throat, nozzle, test section, and diffuser) is cooled by integral, external water jackets. The tunnel is equipped with a model injection system, which allows removal of the model from the test section while the tunnel remains in operation. A description of the tunnel may be found in Ref. 1.

## 2.2 TEST ARTICLES

Three Space Shuttle orbiter models were used to obtain the thin-skin thermocouple data for this test. Two of the test articles were 0.0175 scale models of the full orbiter and were designated as the 60-0 and 56-0 models. The third model was a 0.04 scale of the front half of the orbiter and was identified as the 83-0 model. All of the models were supplied by Rockwell International.

The 60-0 model was a 0.0175 scale thin-skin thermocouple model of the Rockwell International Vehicle 5 configuration. The model was constructed of 17-4 PH stainless steel with a nominal skin thickness of 0.030 in. at the instrumented areas. All thermocouples were spot welded to the thin-skin inner surface.

A photograph of the 60-0 model injected in the tunnel is shown in Fig. 2. A sketch of the 60-0 model installation in the tunnel is shown in Fig. 3. The basic dimensions and coordinate definitions for the 0.0175 scale models are shown in the sketch presented in Fig. 4. The deflection angles of the speedbrake, elevons, and body flaps were all set at zero throughout the test.

The 56-0 model used for this test was model number 2B of the material "LH" 56-0 phase change paint model series. This was a 0.0175 scale model with the same external contour as the 60-0 model. The pilot side of the fuselage consisted of a thin-skin thermocouple insert contoured to the vehicle lines. This insert was constructed of 17-4 stainless steel with a nominal skin thickness of 0.020 in. at the thermocouple locations. A photograph of the 56-0 model injected in the tunnel is shown in Fig. 5. A sketch of the 56-0 model installation is shown in Fig. 6. The dimensions and coordinate system presented in Fig. 4 also apply to the 0.0175 scale 56-0 model.

The 83-0 model was a 0.04 scale model of the forward half of the orbiter. This model was also constructed of 17-4 PH stainless steel with a nominal skin thickness of 0.030 in. A photograph of the 83-0 model in the installation tank beneath the test section is shown in Fig. 7. The installation sketch of the 83-0 model is shown in Fig. 8 and the coordinate system and basic dimensions for the 83-0 model are presented in Fig. 9.

## 2.3 TEST INSTRUMENTATION

### 2.3.1 Test Conditions

The instrumentation, recording devices, and calibration methods used to measure the primary tunnel and test data parameters are listed in Table 2a along with the estimated measurement uncertainties. The range and estimated uncertainties for primary parameters that were calculated from the measured parameters are listed in Table 2b.

### 2.3.2 Test Data

The 60-0 model was instrumented with 600 thirty-gauge iron-constantan and Chromel®-constantan thermocouples. Only 250 of these thermocouples were used on this test. Thermocouple locations for this model are presented in Fig. 10; the dimensional locations and skin thickness for the thermocouples connected on this test are listed in Table 3. The thermocouples identified by a number only are iron-constantan. The thermocouples identified by a number followed by the letter A or C are Chromel-constantan that were added to the model. The letter D after a thermocouple number designates an iron-constantan thermocouple in a new location on the OMS pod.

The 56-0 model instrumentation consisted of 80 thirty-gauge Chromel-constantan thermocouples located on the thin skin insert. All of these thermocouples were connected on this test. The thermocouple locations for this model are presented in Fig. 11. The dimensional locations and skin thicknesses are listed in Table 4.

For this test only 250 of the 482 thirty-gauge Chromel-constantan thermocouples on the 83-0 model were connected. The thermocouple locations for this model are illustrated in Fig. 12. The dimensional locations and skin thicknesses for the thermocouples used on this test are listed in Table 5.

## 3.0 TEST DESCRIPTION

### 3.1 TEST CONDITIONS

A summary of the nominal test conditions at each Mach number is given below:

<u>M</u>	<u>PT, psia</u>	<u>TT, °R</u>	<u>Q, psia</u>	<u>P, psia</u>	<u>RE x 10<sup>-6</sup>, ft<sup>-1</sup></u>
8	100	1250	0.5	0.010	0.5
8	205	1250	1.0	0.02	1.0
8	.325	1300	1.5	0.035	1.5

A test summary showing the configurations tested and the variables for each is presented in Table 6.

### 3.2 TEST PROCEDURE

#### 3.2.1 General

In the VKF continuous flow wind tunnels (A, B, C), the model is mounted on a sting support mechanism in an installation tank directly underneath the tunnel test section. The tank is separated from the tunnel by a pair of fairing doors and a safety door. When closed, the fairing doors, except for a slot for the pitch sector, cover the opening to the tank and the safety door seals the tunnel from the tank area. After the model is prepared for a data run, the personnel access door to

the installation tank is closed, the tank is vented to the tunnel flow, the safety and fairing doors are opened, and the model is injected into the airstream. After the data are obtained, the model is retracted into the tank and the sequence is reversed with the tank being vented to atmosphere to allow access to the model in preparation for the next run. A given injection cycle is termed a run, and all the data obtained are identified in the data tabulations by a run number.

### 3.2.2 Thin-Skin Thermocouple

Prior to each test run, the model temperatures were monitored to ensure that the model was nominally isothermal. The model was then injected at the desired test attitude as the data acquisition sequence commenced. The model remained on the tunnel centerline for about three seconds and was then retracted into the installation tank. The model was then cooled while being repositioned for the next injection.

A 256 channel multiplexing analog-to-digital converter was used in conjunction with a Digital Equipment Corporation (DEC) PDP-11 computer and a DEC-10 computer to record the temperature data. The system sampled the output of each thermocouple approximately 13 times per second.

### 3.2.3 Oil-Flow

Oil-flow testing was done on the 60-0 model and the 83-0 model. For oil-flow testing the models were painted black for contrast, and in general, a white oil with a viscosity of 25 centistokes was applied to the surface with a sponge for each run. The oil was applied differently on the first two runs of the 83-0 model. On runs 77 and 78, coatings of 800-centistoke and 200-centistoke white oil were applied over a coating of clear Dow Corning oil with a viscosity of 100 centistokes. The model was positioned to the test attitude and injected into the tunnel flow for about 20 sec. During this time, four still cameras photographed the model at 2-second intervals. Locations of the cameras and camera numbers are specified in Table 7. After the model was retracted from the tunnel flow, it was cooled and cleaned before oil was reapplied for the next test run. Oil flow runs are specified in the Test Data Summary, Table 6.

## 3.3 DATA REDUCTION

### 3.3.1 Thin-Skin Thermocouple Data

The reduction of thin skin temperature data to coefficient form normally involves only the calorimeter heat balance for the thin skin as follows:

$$QDOT = \rho bc DTW/DT \quad (1)$$

$$H(TR) = \frac{QDOT}{TR-TW} = \frac{\rho bc DTW/DT}{TR-TW} \quad (2)$$

Thermal radiation and heat conduction effects on the thin-skin element are neglected in the above relationship and the skin temperature

response is assumed to be due to convective heating only. It can be shown that for constant TR, the following relationship is true:

$$\frac{d}{dt} \ln \left[ \frac{TR-TI}{TR-TW} \right] = \frac{DTW/DT}{TR-TW} \quad (3)$$

Substituting Eq. (3) in Eq. (2) and rearranging terms yields:

$$\frac{H(TR)}{\rho bc} = \frac{d}{dt} \ln \left[ \frac{TR-TI}{TR-TW} \right] \quad (4)$$

By assuming that the value of  $H(TR)/\rho bc$  is a constant, one can see that the derivative (or slope) must also be constant. Hence, the term

$$\ln \left[ \frac{TR-TI}{TR-TW} \right]$$

is linear with time. This linearity assumes the validity of Eq. (2) which applies for convective heating only. The evaluation of conduction effects will be discussed later.

The assumption that  $H(TR)$  and  $c$  are constant are reasonable for this test although small variations do occur in these parameters. The variations of  $H(TR)$  caused by changing wall temperature and by transition movement with wall temperature are trivial for the small wall temperature changes that occur during data reduction. The value of the model material specific heat,  $c$ , was computed by the relation

$$c = 0.0797 + (5.556 \times 10^{-5})TW \quad (17-4 \text{ PH stainless steel}) \quad (5)$$

The maximum variation of  $c$  over any curve fit was less than 1.5 percent. Thus, the assumption of constant  $c$  used to derive Equation 4 was reasonable. The value of density used for the 17-4 PH stainless steel skin was  $\rho = 490 \text{ lbm/ft}^3$ , and the skin thickness,  $b$ , for each thermocouple is listed in Tables 3, 4 or 5.

The right side of Equation 4 was evaluated using a linear least squares curve fit of 15 consecutive data points to determine the slope. The curve fit was started at approximately the time the model arrived on the tunnel centerline. For each thermocouple the tabulated value of  $H(TR)$  was calculated from the slope and the appropriate values of  $\rho bc$ ; i.e.,

$$H(TR) = \rho bc \frac{d}{dt} \ln \left[ \frac{TR-TI}{TR-TW} \right] \quad (6)$$

To investigate conduction effects a second value of  $H(TR)$  was calculated at a time one second later. A comparison of these two values was used to identify those thermocouples that were influenced by significant conduction (or system noise). The data for a given thermocouple were deleted\* if these values of  $H(TR)$  differed by more than 35 percent. In general, conduction and/or noise effects were found to be negligible.

Since the value of  $TR$  is not known at each thermocouple location it has become standard procedure to use three assumed values of  $TR$ . The assumed values are  $1.0TT$ ,  $0.9TT$  and  $0.85TT$ . The use of these assumed values of  $TR$  provides an indication of the sensitivity of the heat-transfer coefficients to the value of  $TR$  assumed. As can be noted in the tabulated data, there are large percentage differences in the values of the heat-transfer coefficients calculated from the three assumed values. Therefore, if the data are to be used for flight predictions, the value selected for  $TR$  is obviously very important and is a function of model location and boundary layer state.

The heat-transfer coefficient calculated from Eq. 4 was normalized using the Fay-Riddell stagnation point coefficient,  $H(REF)$ , based on a nose radius of 1.0 ft full scale (see Appendix III). The reference nose radius,  $RN$ , used to calculate  $H(REF)$  is either 0.0175 ft or 0.04 ft as determined by the model scale.

#### 3.4 UNCERTAINTY OF MEASUREMENTS

In general, instrumentation calibrations and data uncertainty estimates were made using methods recognized by the National Bureau of Standards (NBS). Measurement uncertainty is a combination of bias and precision errors defined as:

$$U = \pm (B + t_{95}S)$$

where  $B$  is the bias limit,  $S$  is the sample standard deviation and  $t_{95}$  is the 95th percentile point for the two-tailed Student's "t" distribution (95-percent confidence interval), which for sample sizes greater than 30 is taken equal to 2.

Estimates of the measured data uncertainties for this test are given in Table 2a. The data uncertainties for the measurements are determined from in-place calibrations through the data recording system and data reduction program.

Propagation of the bias and precision errors of measured data through the calculated data was made in accordance with Ref. 2 and the results are given in Table 2b.

---

\*The word DELETE is used on the tabulated data to identify these thermocouples.



#### 4.0 DATA PACKAGE PRESENTATION

Heat-transfer coefficients were obtained at selected locations on the 56-0, 60-0, and 83-0 models of the space shuttle orbiter. Sample tabulated data are presented in Appendix IV.

Representative data from the upper centerline ( $\text{PHI} = 180$  deg) of the 83-0 model are presented in Fig. 13. Data from two runs are presented as a sample of data repeatability.

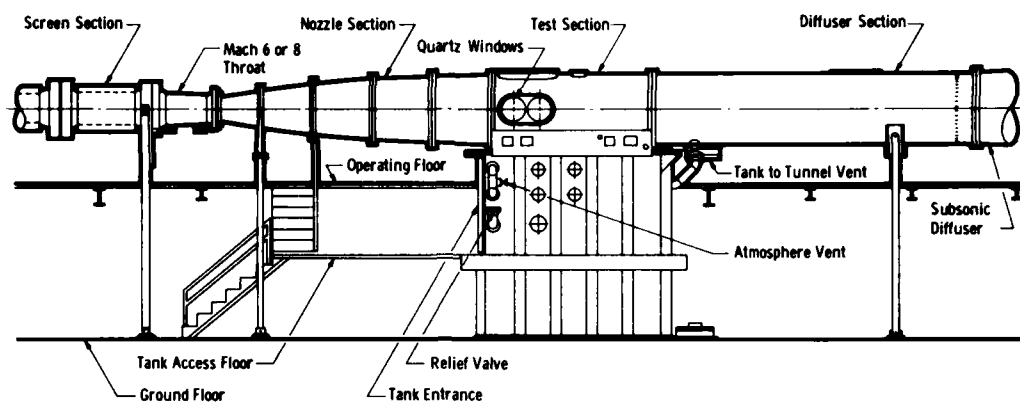
Representative oil-flow data of the 60-0 model are shown in Fig. 14.

#### REFERENCES

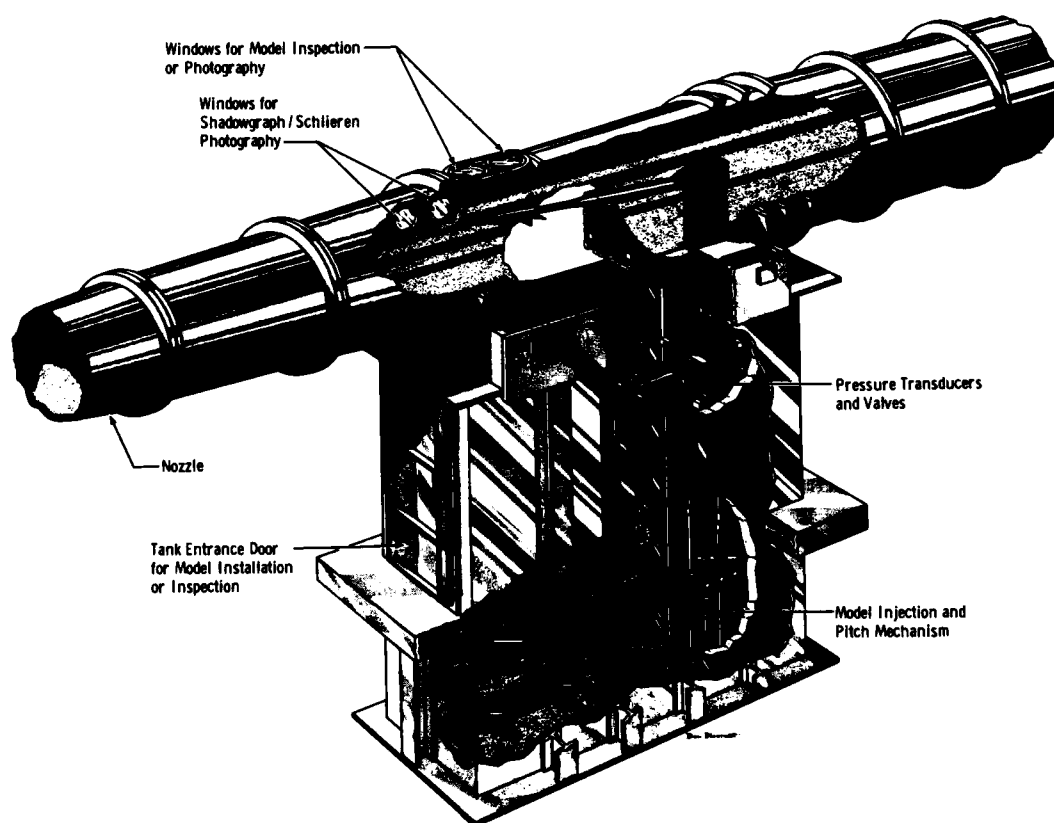
1. Test Facilities Handbook (Eleventh Edition). "von Karman Gas Dynamics Facility, Vol. 3." Arnold Engineering Development Center, June 1979.
2. Thompson, J. W. and Abernethy, R. B. et al. "Handbook Uncertainty in Gas Turbine Measurements." AEDC-TR-73-5 (AD755356), February 1973.

APPENDIX I

ILLUSTRATIONS



a. Tunnel assembly



b. Tunnel test section  
Fig. 1. Tunnel B



A E D C  
7602-81

Figure 2. Installation Photograph of 60-0 Model

# 50-INCH HYPERSONIC TUNNELS B&C

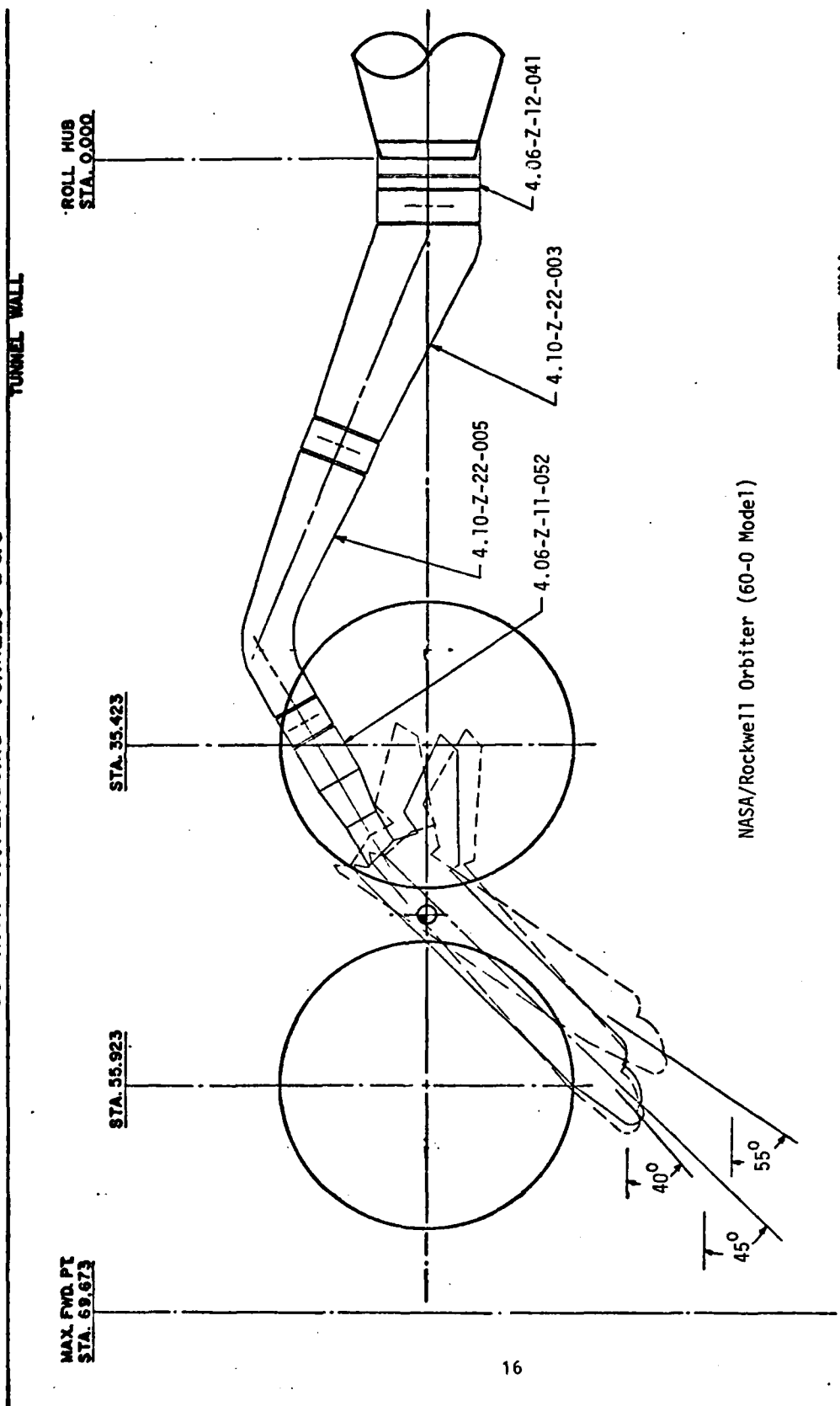


Figure 3. 60-0 Model Installation

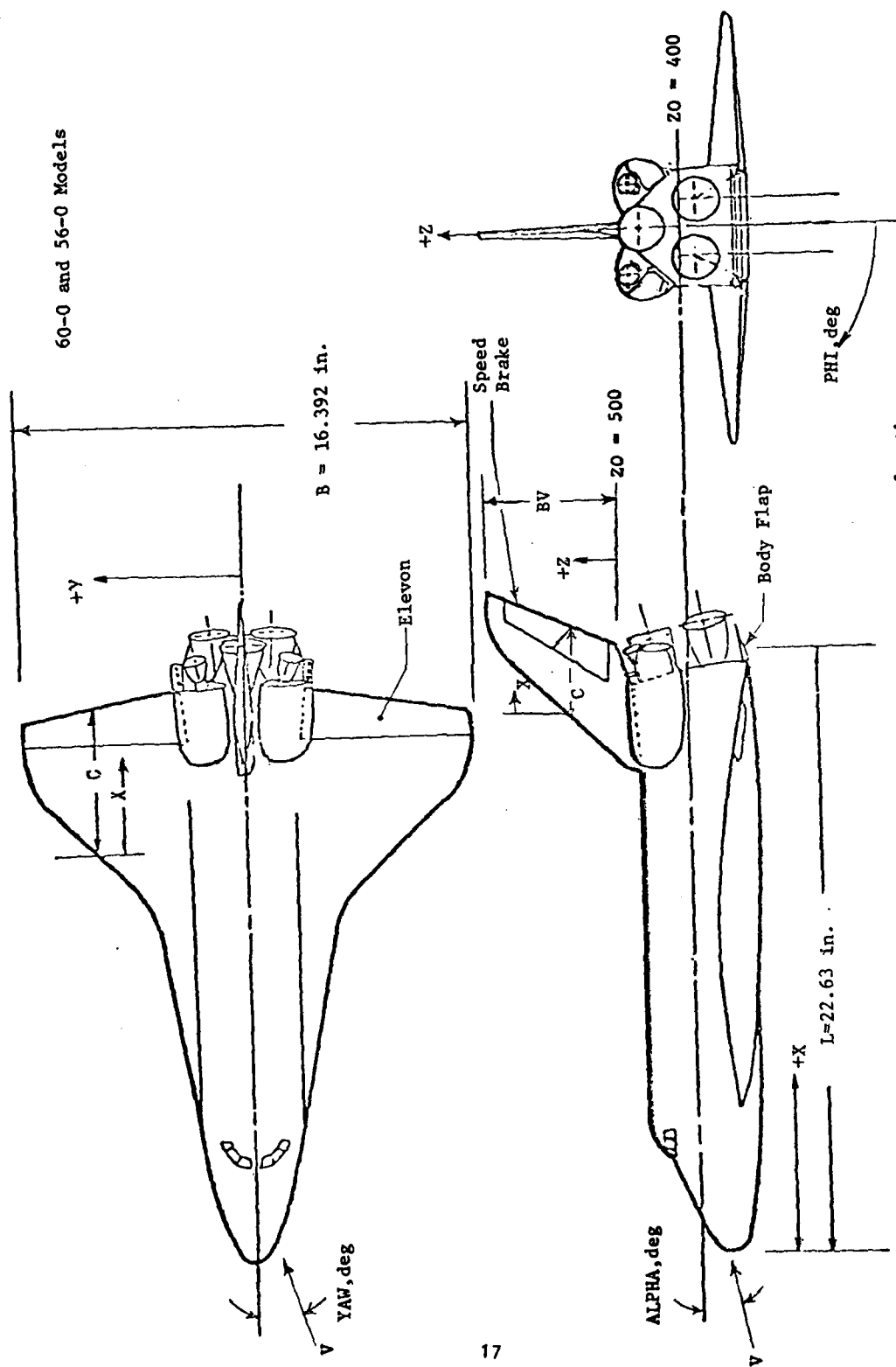


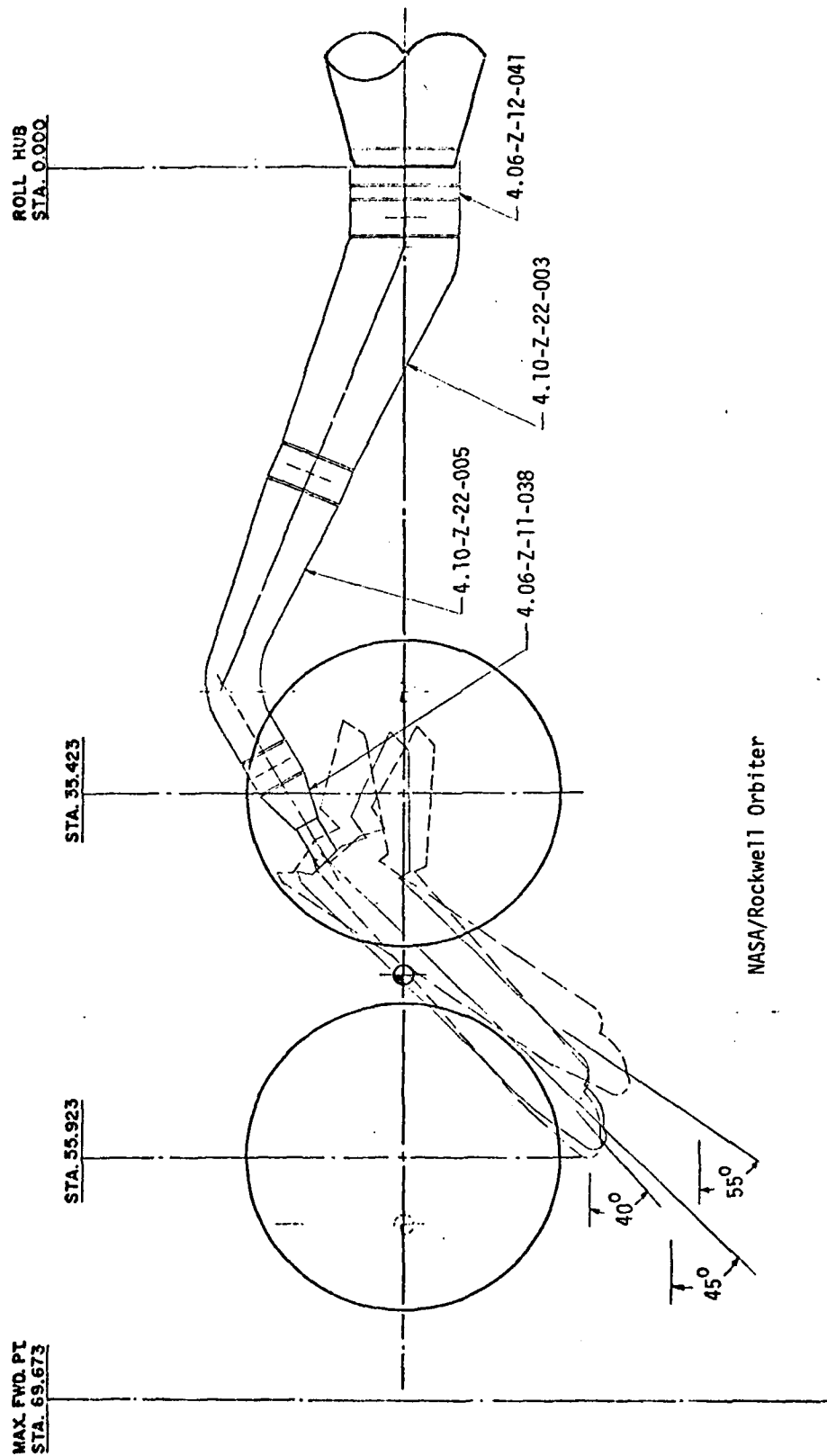
Fig. 4. Basic Dimensions and Coordinate System for the 0.0175 Scale Orbiter Models



Figure 5. Installation Photograph of 56-0 Model

# 50-INCH HYPERSONIC TUNNELS B&C

TUNNEL WALL



TUNNEL WALL

Figure 6. 56-0 Model Installation



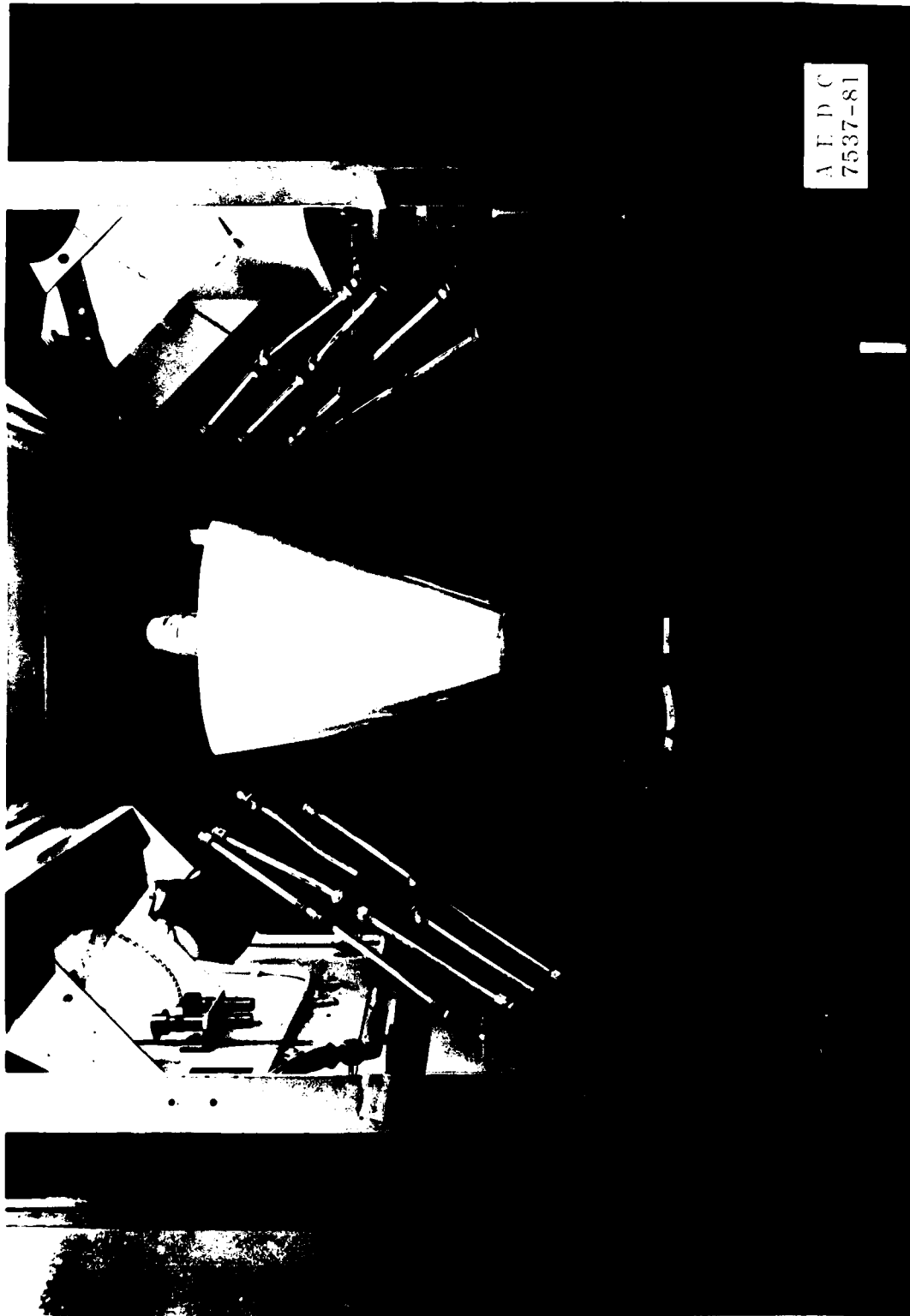


Figure 7. Installation Photograph of 83-0 Model

# 50-INCH HYPERSONIC TUNNELS B&C

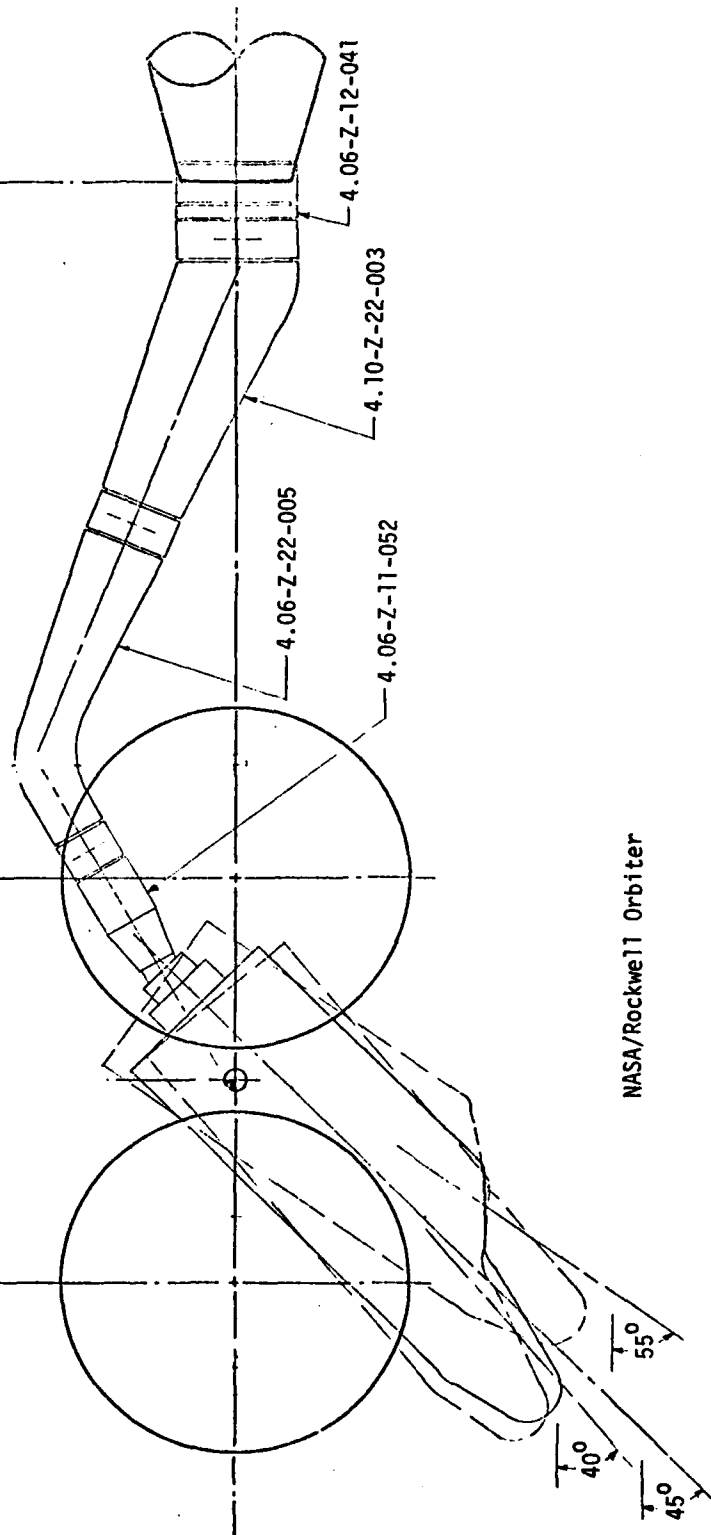
TUNNEL WALL

MAX. FWD. PT.  
STA. 69.673

STA. 55.923

STA. 35.423

ROLL HUB  
STA. 0.000



21

TUNNEL WALL

Figure 8. 83-0 Model Installation

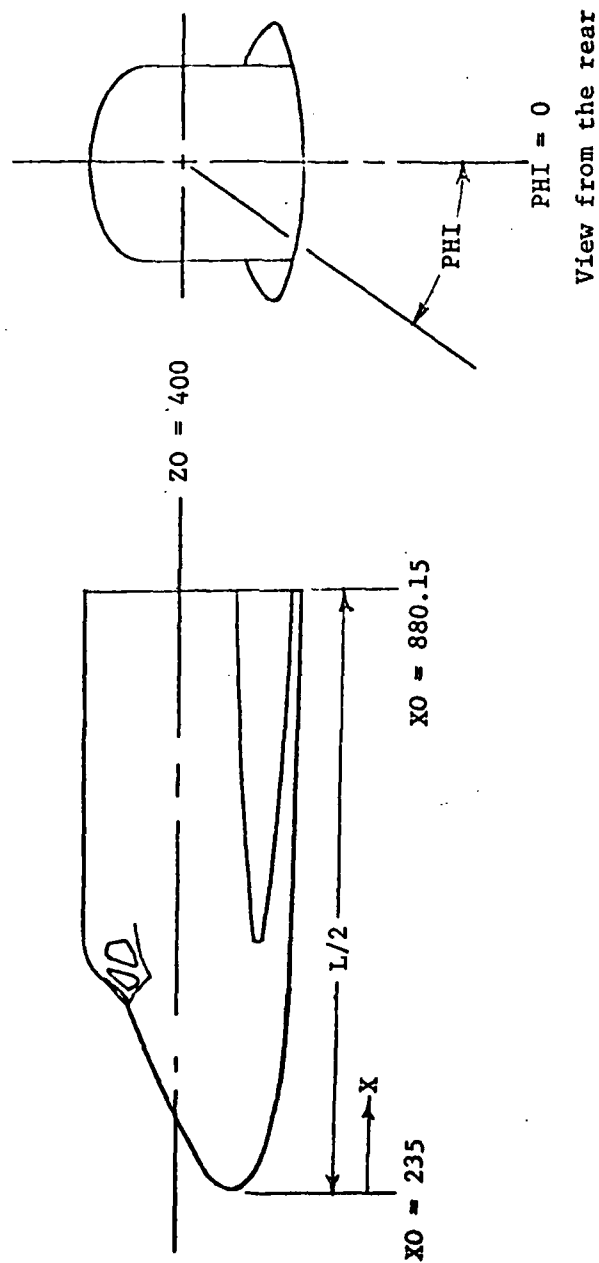
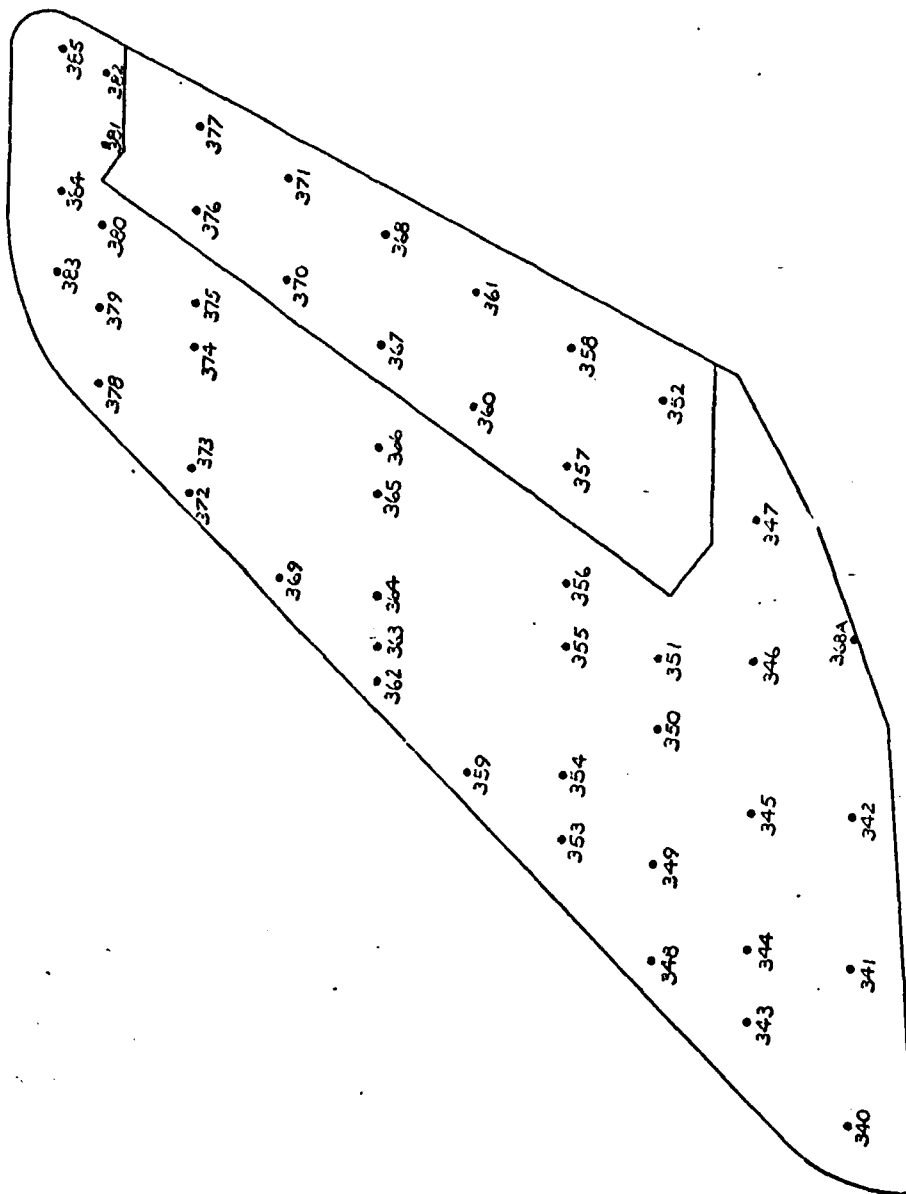
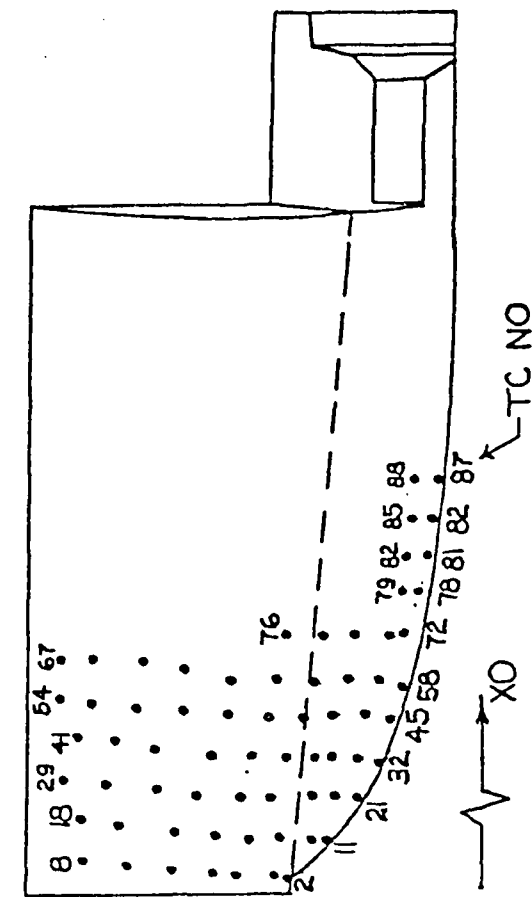


Fig. 9. Basic Dimensions and Coordinate System for the  
83-0 Model



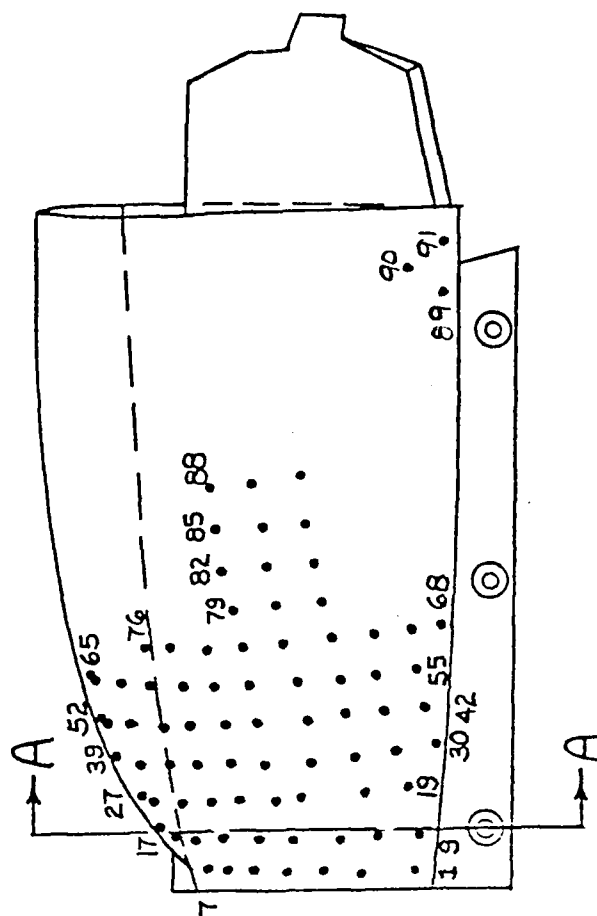
a. Vertical Tail

Fig. 10. Thermocouple Locations on 60-0 Model

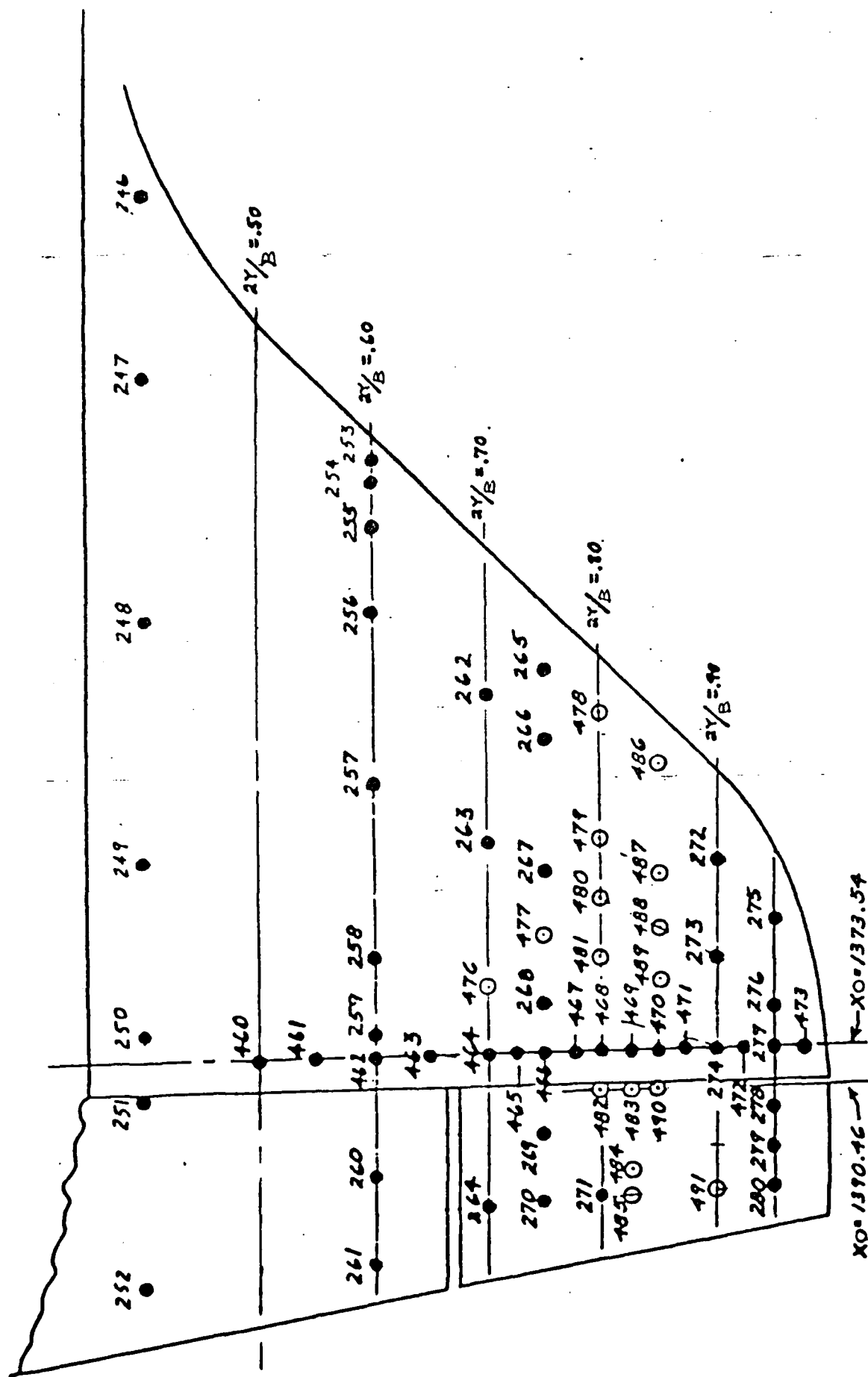


# SECTION A-A

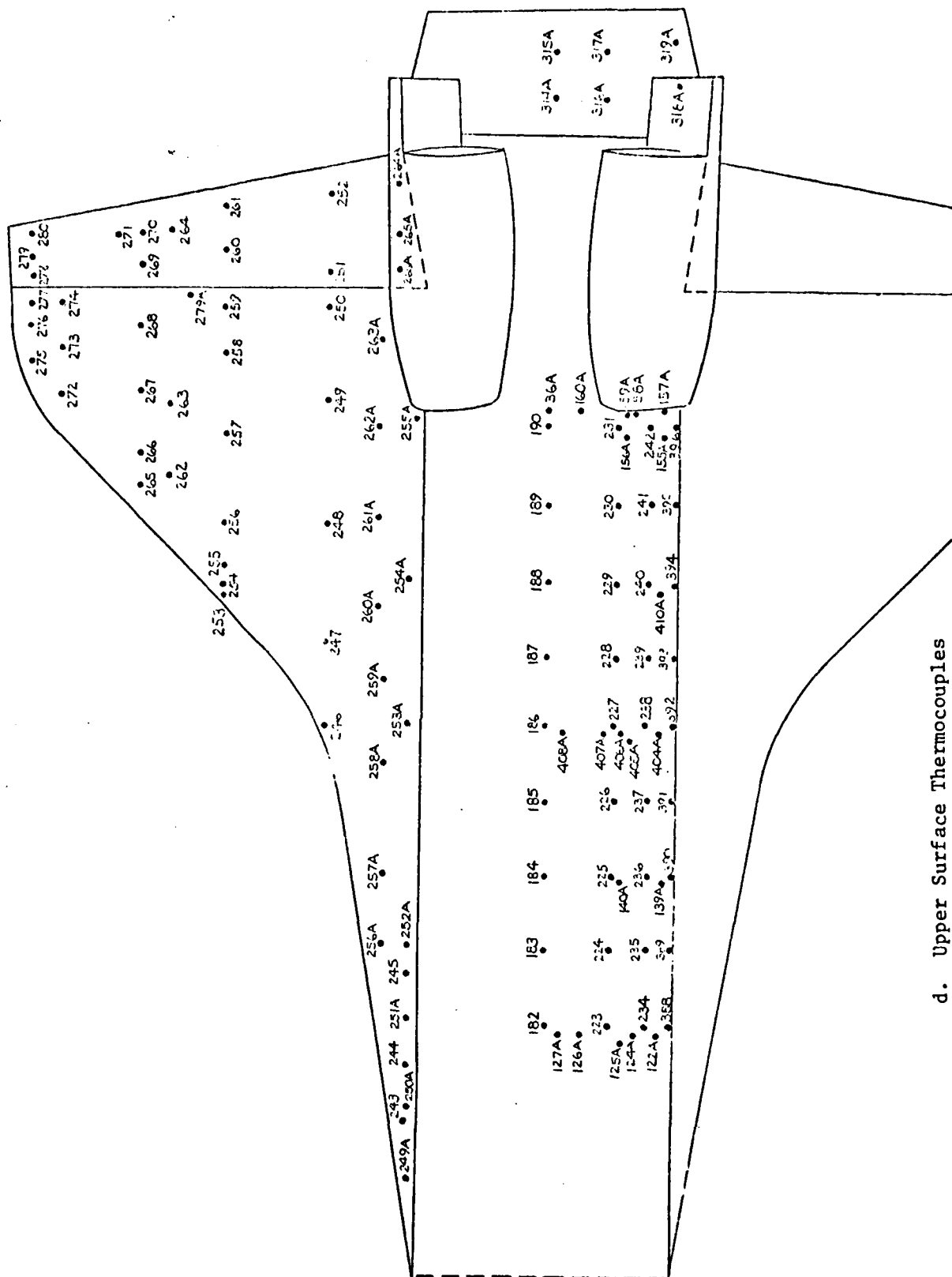
NOTE: FOR CLARITY, NOT ALL TC NOS. SHOWN



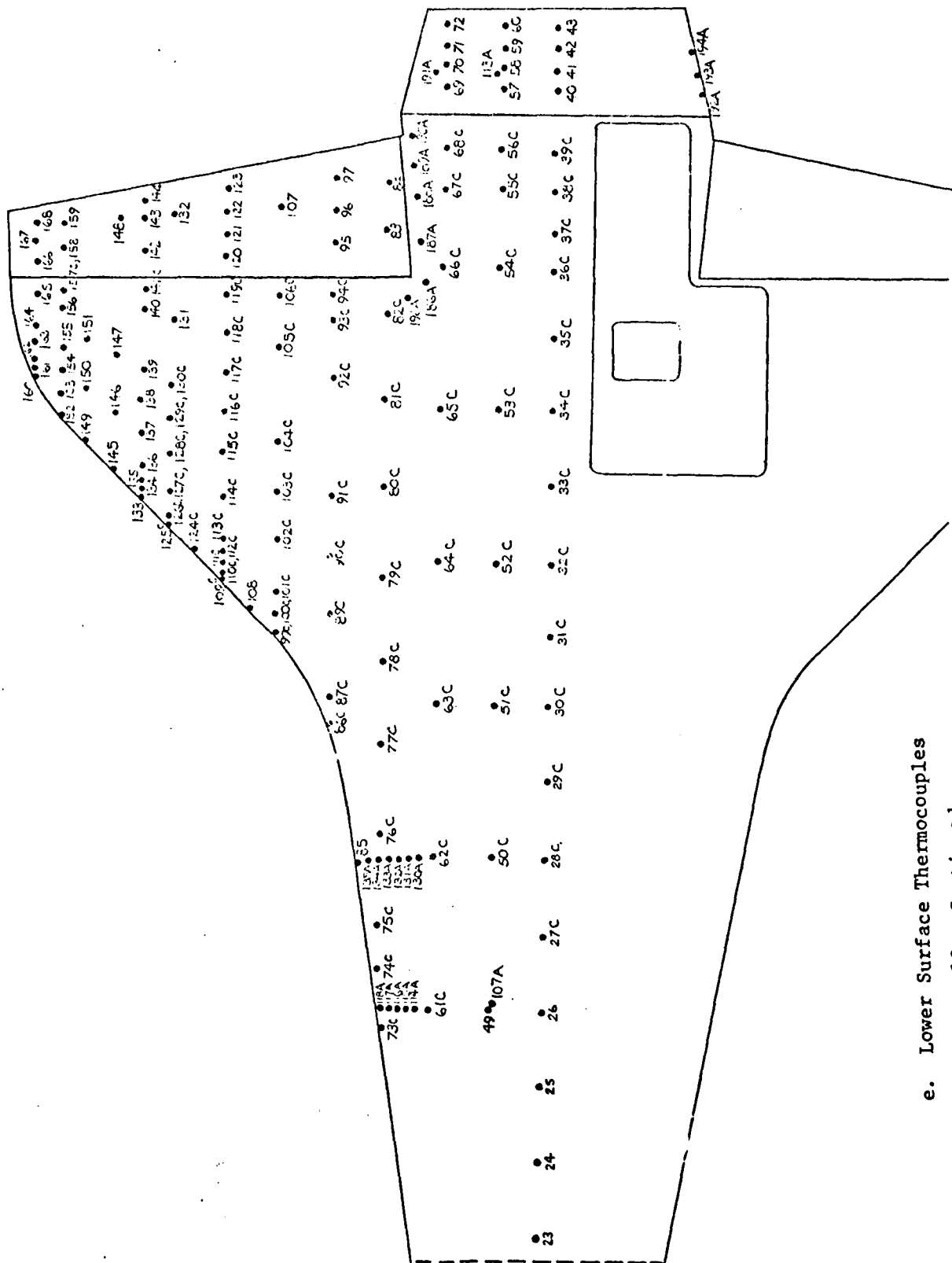
b. OMS Pod Thermocouple Locations  
Fig. 10. Continued



c. Upper Right Wing  
Fig. 10. Continued



d. Upper Surface Thermocouples  
Fig. 10. Continued



e. Lower Surface Thermocouples  
Fig. 10. Continued





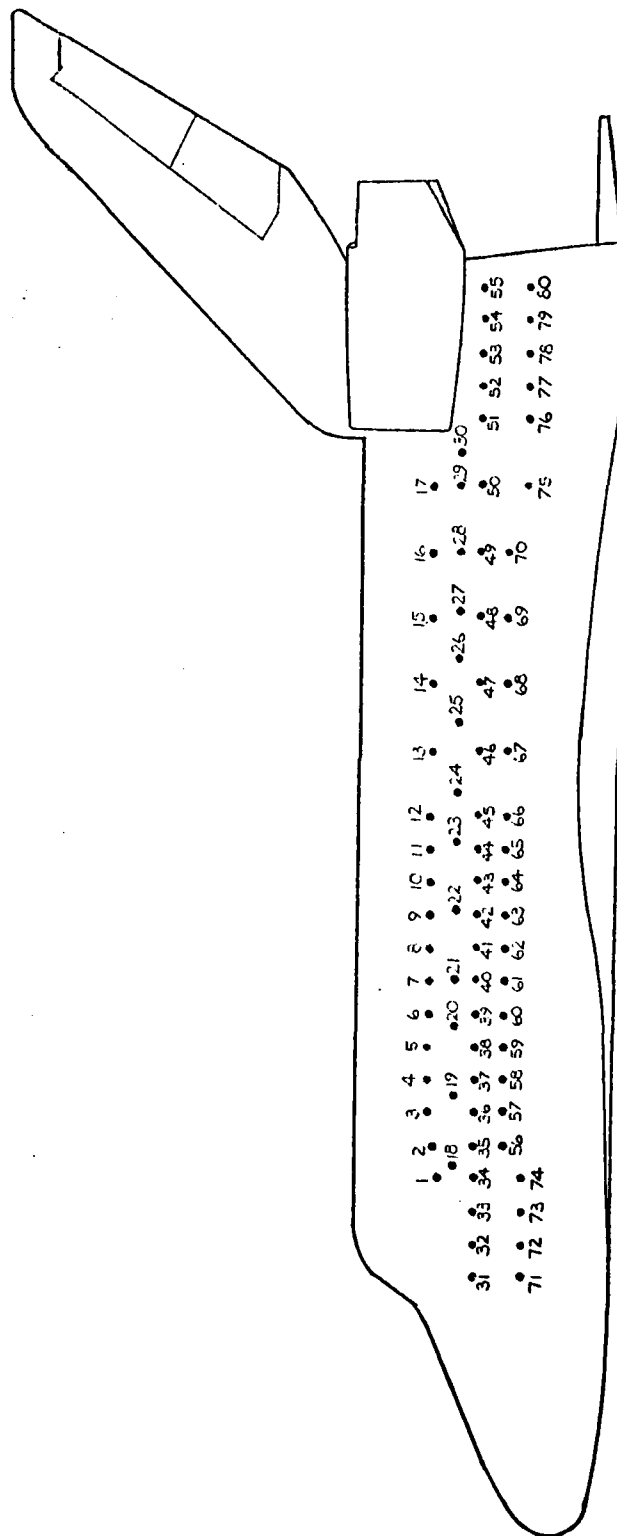
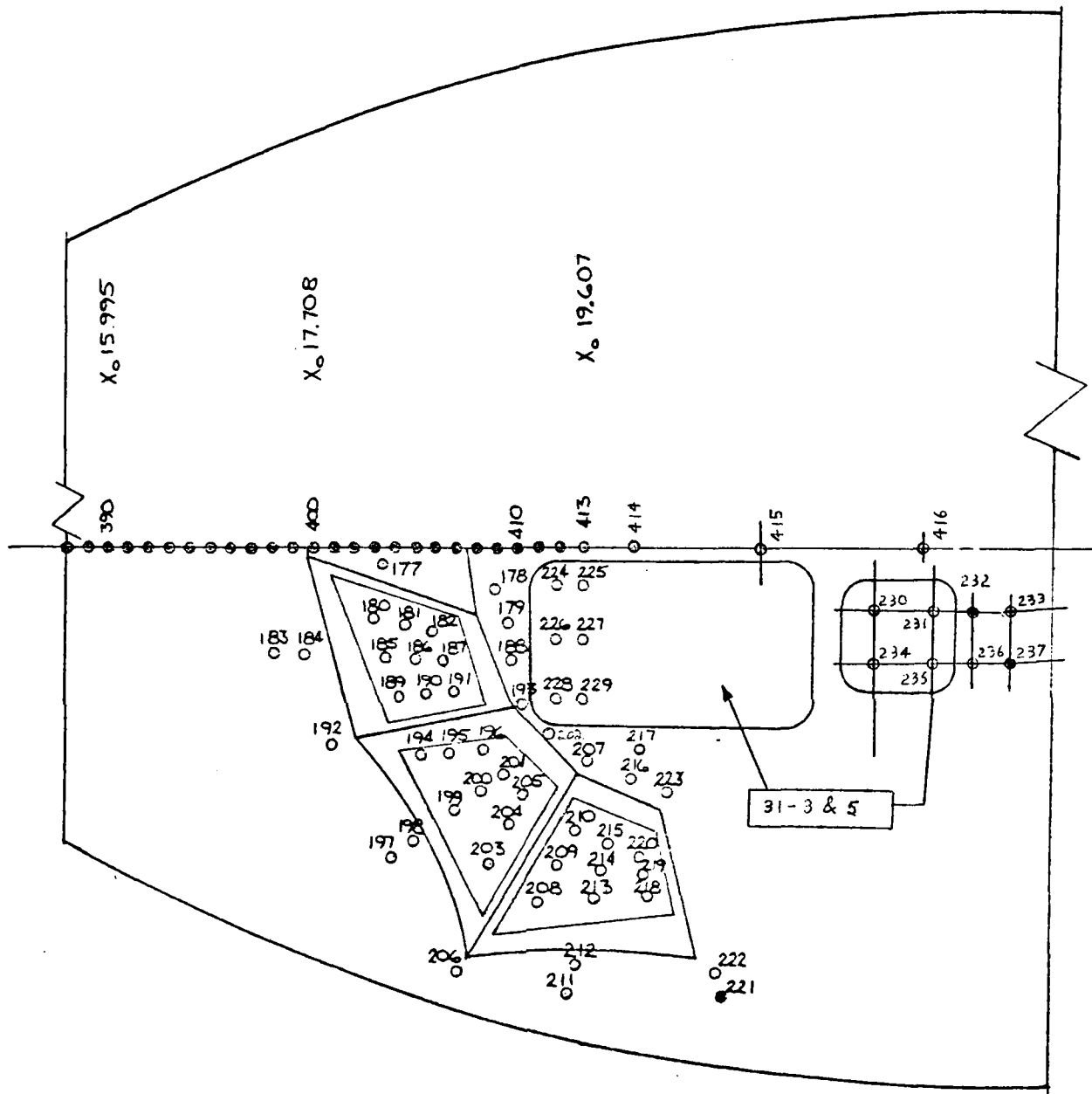
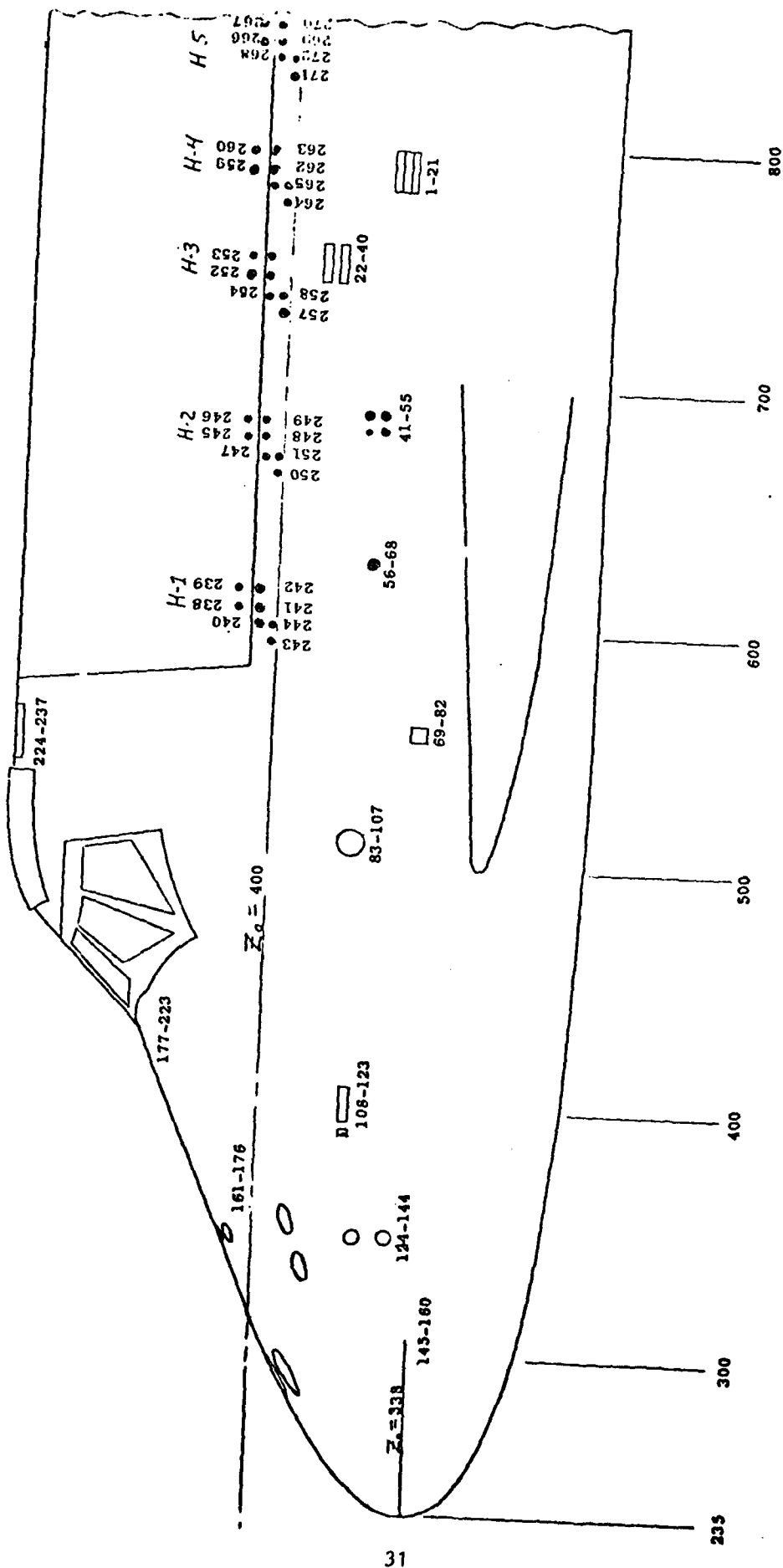


Fig. 11. Thermocouple Locations on 56-O Model

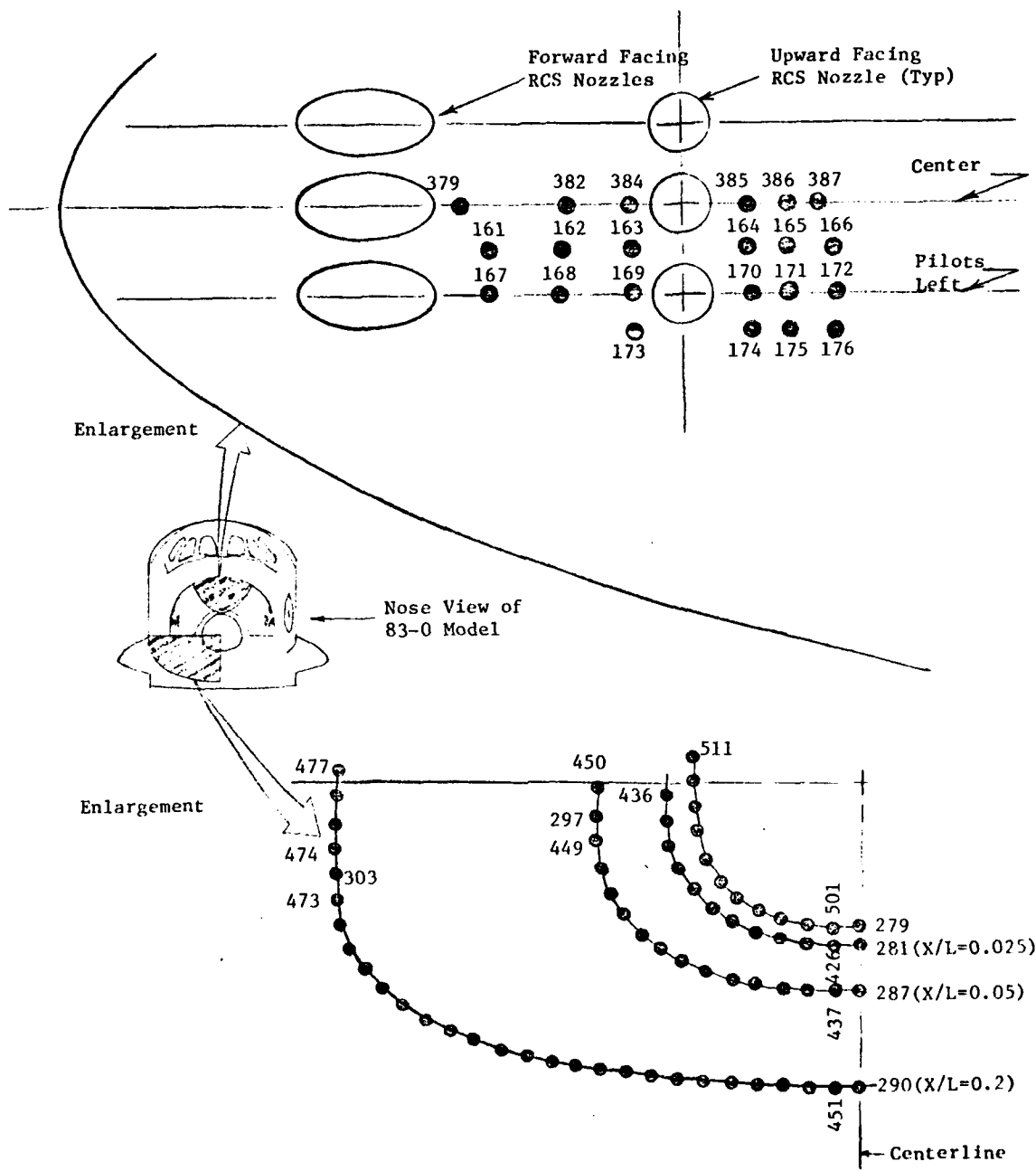


a. Canopy Thermocouple Locations  
 Fig. 12. Thermocouple Locations on 83-0 Model

MODEL 83-0  
(Pilot Side)

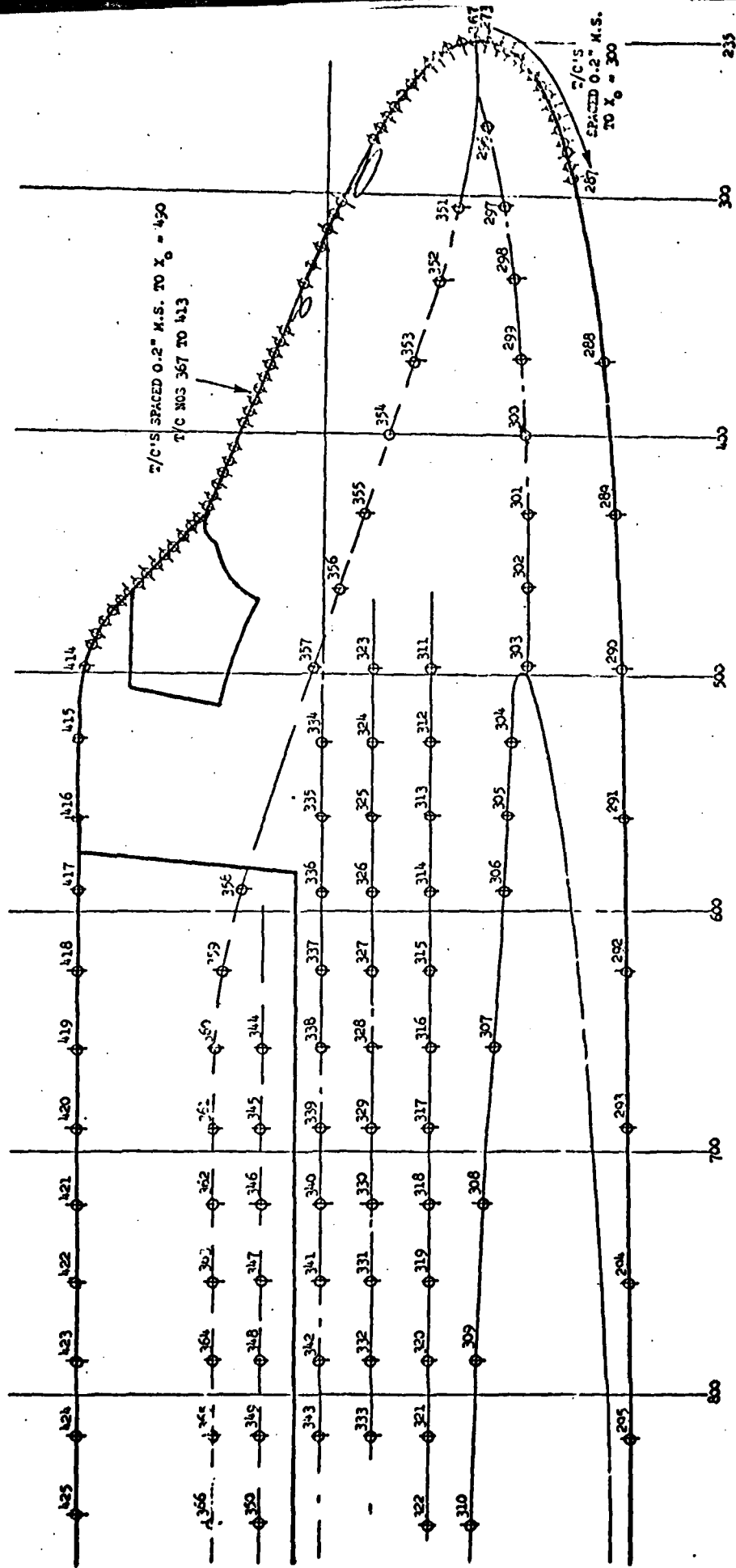


b. Thermocouple Locations on the Pilot Side  
Fig. 12. Continued



c. Thermocouple Locations on Upper RCS Nozzles and Lower Fuselage

Figure 12. Continued



d, Thermocouple Locations on the Copilot Side

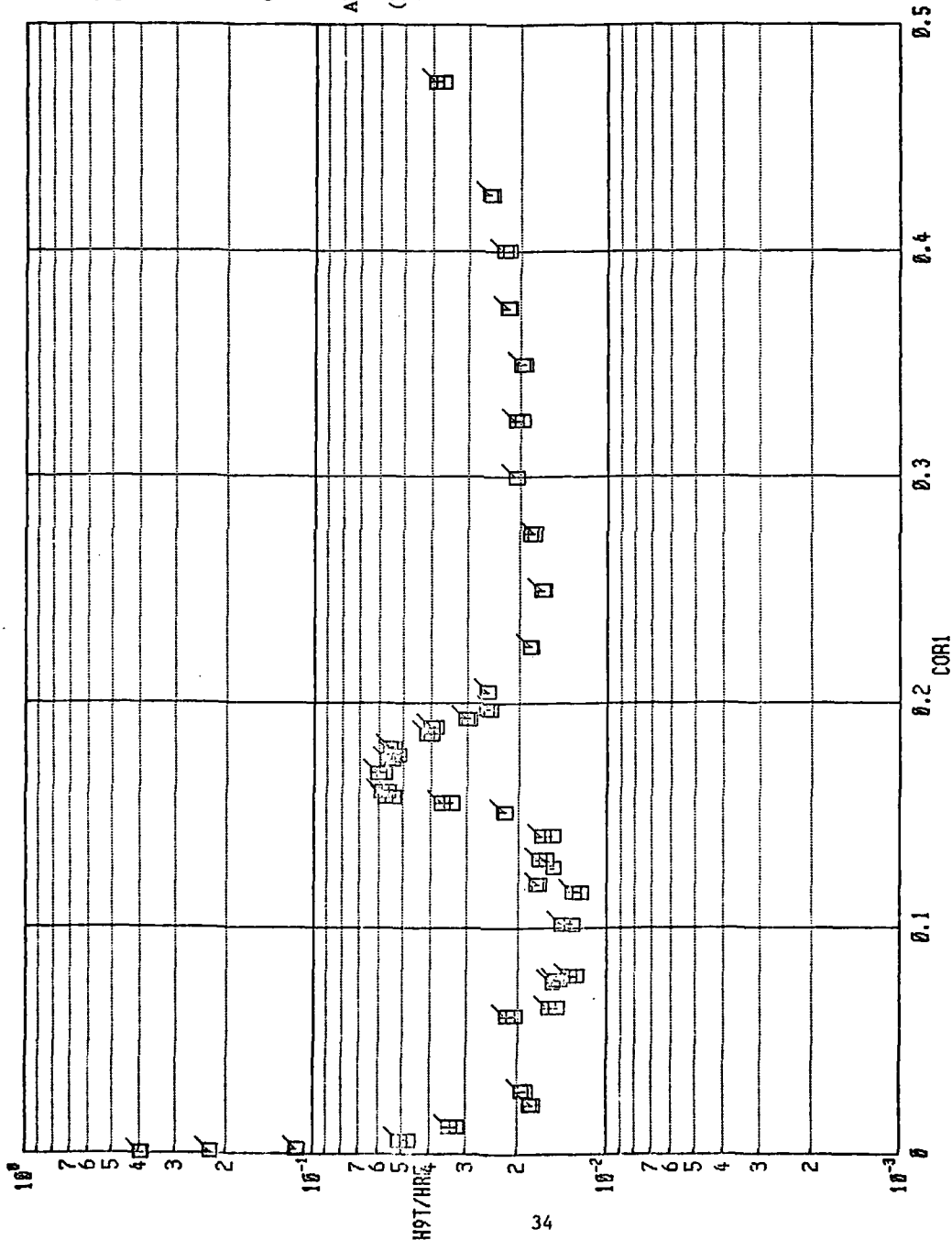
Fig. 12. Concluded

83-0 Model Upper  
Centerline Data

TC NO.  
367-425

Conditions:

M = 8  
RE =  $1.5 \times 10^6 \text{ ft}^{-1}$   
ALPHA = 55 deg  
YAW = 0 deg  
(Runs 44 and 76 are  
repeat runs.)



PRE 2  
27-OCT-81  
11:58

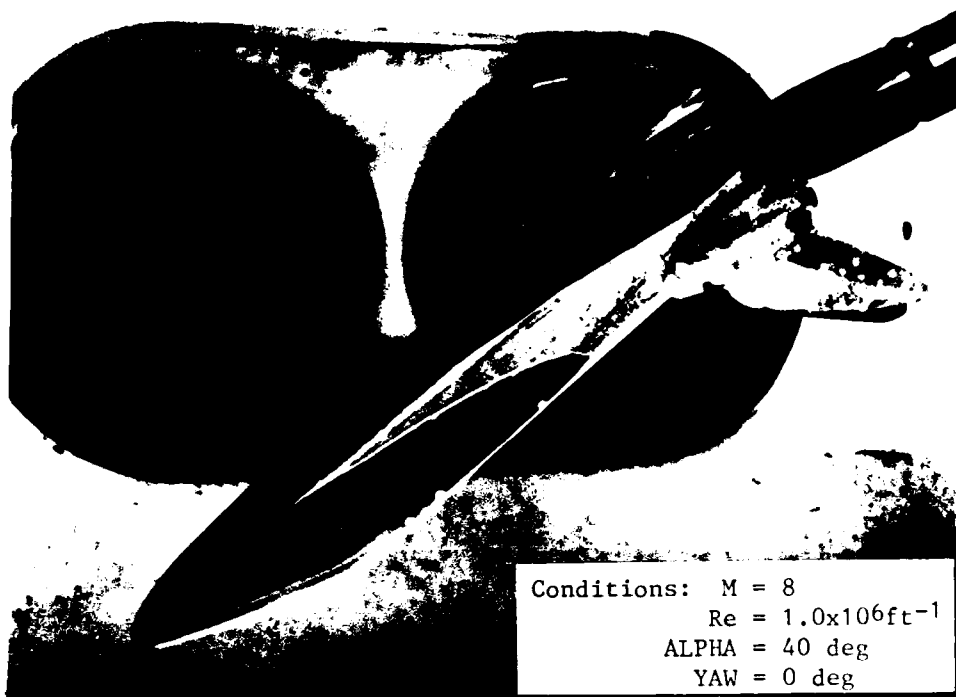
RUN 44 076

NASA/RI OH111 HEATING

Figure 13. Thin-Skin Thermocouple Plotted Data



Camera 2



Conditions:  $M = 8$   
 $Re = 1.0 \times 10^6 ft^{-1}$   
 $\alpha = 40 \text{ deg}$   
 $\gamma = 0 \text{ deg}$



Camera 3

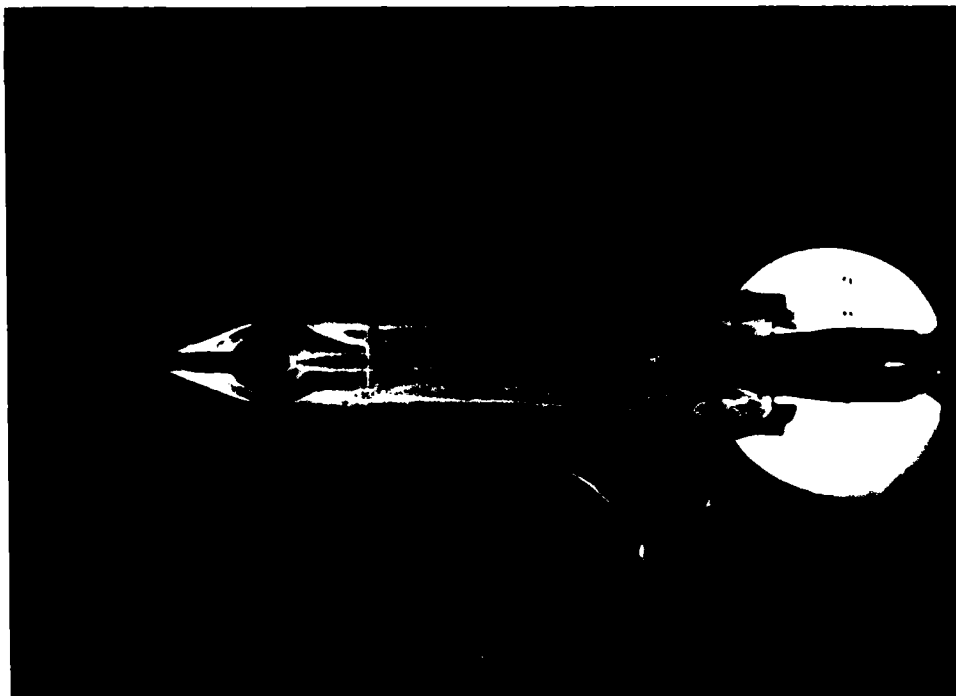


Figure 14. Oil-Flow Photographs on 60-0 Model (Run 262)



APPENDIX II

TABLES

TABLE 1. Data Transmittal Summary

The following items were transmitted:

Item	No. of Copies	No. of Copies	No. of Copies	No. of Copies	No. of Copies
Mrs. Dorothy B. Lee NASA Johnson Space Center ES3 Houston, TX 77058	1				Mr. R. D. Neumann AFWAL/FING Wright-Patterson AFB, OH 45433
Mr. J. Gee Rockwell International Space Transportation and Systems Group Mail Code AC07 12214 Lakewood Blvd. Downey, CA 90241	3				Mr. E. K. Hertzler 6510 TESTW/TEG Stop 236 Edwards AFB, CA 93523
Mr. Don Poucher Chrysler Corp. Space Division P. O. Box 29200 Dept. 2734 New Orleans, LA 70189	3				
Test Summary Report	1			1	1
83-0 Model: Heat Transfer and Oil Flow Tabulated Data (Runs 1-81)	1	3		1	1
56-0 Model: Heat Transfer Tabulated Data (Runs 82-171)	1	3		1	1
60-0 Model: Heat Transfer and Oil Flow Tabulated Data (Runs 172-269) Vols. 1 and 2 of 2	1	3		1	1
Magnetic Tape: Data from 83-0 56-0 and 60-0 (Runs 1-269)			1		
70 mm Schlieren Stills: Contact Prints and Duplicate Negatives (Runs 1-269)		1			
70 mm Oil Flow Stills: Contact Prints and Duplicate Negatives, 83-0 (Runs 77-81, Rolls 627, 630, 687, 699), 60-0 (Runs 262-269, Rolls 716, 781, 792, 786)					

TABLE 2. ESTIMATED UNCERTAINTIES

## a. Basic Measurements

Parameter Designation	STEADY-STATE ESTIMATED MEASUREMENT*							Range	Type of Measuring Device	Type of Recording Device	Method of System Calibration
	Precision Index $\pm(S)$		Bias $\pm(B)$		Uncertainty $\pm(B + t_{95S})$						
	Percent of Reading	Unit of Measurement	Degree of Freedom	Percent of Reading	Unit of Measurement	Percent of Reading	Unit of Measurement				
ALPI, deg PHI, deg		0.025	> 30			0.05	$\pm 11$	Potentiometer	Analog-to-digital converter into data acquisition system	Heidenhain rotary encoder Rod700 Resolution: 0.000 Overall accuracy: 0.0010	
		0.15	> 30			0.3	$\pm 90$				
PI, psia		0.02	> 30		0.46	0.3	0-P $\leq 104$	Bell & Howell variable capacitance pressure transducer	Analog to Digital Converter into Data Acquisition System	in-place application of multiple pressure levels measured with a pressure measuring device calibrated in the standards laboratory	
		0.11	> 30	0.25		$\pm(0.25\% + .08 \text{ psi})$	104-P $\leq 200$				
		0.11	> 30	0.25	0.58	0.80	200-P $\leq 232$				
						$\pm(0.25\% + 0.22 \text{ psi})$	232-P $\leq 1000$				
TIME, sec		$5 \times 10^{-4}$	> 30	$\left[ \frac{\text{Runtime in sec}}{(5 \times 10^{-6})} \right]$		$\pm \left[ \frac{\text{Runtime in sec}}{(5 \times 10^{-6})} \right]$	milli-seconds to 365 days	Syston Donner time code reader	Digital Data Acquisition System	Instrument lab calibration against NES	
TT, °F	1		> 30	0.375		$\pm(0.375\% + 2^{\circ}\text{F})$	790-890	Chromel <sup>®</sup> -Alumel <sup>®</sup> Thermocouple	Digital Thermometer into Digital Data Acquisition System	Thermocouple verification of NES conformity/voltage substitution calibration	
TW, °F	1		> 30		2	4	50-200	FE-CN Thermocouple	Low Level Multiplexer into Analog to Digital Converter into Data Acquisition System		
	1		> 30		2	4	50-200	CR-CN Thermocouple			

\*Thompson, J. W. and Abernethy, R. B.: et al. "Handbook Uncertainty in Gas Turbine Measurements." AEDC-TR-73-5 (AD 755356), February 1973.

TABLE 2. Concluded

## b. Calculated Parameters

Parameter Designation	STEADY-STATE ESTIMATED MEASUREMENT*							
	Precision Index $\pm(S)$			Bias $\pm(B)$		Uncertainty $\pm(B + t_{95S})$		Range
	Percent of Reading	Unit of Measurement	Degree of Freedom	Percent of Reading	Unit of Measurement	Percent of Reading	Unit of Measurement	
M		0.020 0.010	>30		0+		0.04 0.02	7.83 8.0
RE, ft <sup>-1</sup>	0.70 0.36		>30	0.56 0.45		1.96 1.17		$0.5 \times 10^6 \text{ ft}^{-1}$ $3.7 \times 10^6 \text{ ft}^{-1}$
H(TT), H(-9TT), 2 H(-85TT), BTU/ft <sup>2</sup> - sec-OR (Thin-skin thermo- couple technique)	1.0 4.0 7.0		>30	6.0 6.0 6.0		4.0 14.0 20.0		$> 1 \times 10^{-3}$ $1 \times 10^{-1}$ $1 \times 10^{-3}$ $< 1 \times 10^{-4}$

\*Abernethy, R. B. et al. and Thompson, J. W. "Handbook Uncertainty in Gas Turbine Measurements." AEDC-TR-73-5 (AD 756356), February 1973.  
 +Assumed to be zero

TABLE 3. 60-0 Model Thermocouple Coordinates

Vertical Tail				Vertical Tail				OMS Pod				
T/C	X/C	Z/BV	b, in.	T/C	X/C	Z/BV	b, in.	T/C	XO, in.	YO, in.	ZO, in.	b, in.
340	0.1	0.1	0.032	375	0.5	0.8	0.033	26D	1339.9	76.58	512.79	0.030
341	0.3	0.1	0.031	376	0.7	0.8	0.028	27D	1341.3	64.09	517.49	0.026
342	0.5	0.1	0.030	379	0.3	0.9	0.031	28D	1343.2	50.13	514.51	0.030
343	0.2	0.2	0.030	381	0.7	0.5	0.031	29D	1344.6	38.66	506.42	0.029
345	0.4	0.2	0.031	382	0.9	0.9	0.030	30D	1348.9	111.69	427.05	0.015
346	0.6	0.2	0.031	384	0.5	0.95	0.032	31D	1348.0	119.71	438.95	0.023
347	0.8	0.2	0.032	385	0.9	0.95	0.033	32D	1346.9	126.40	451.59	0.029
349	0.2	0.3	0.031									
350	0.4	0.3	0.031					34D	1347.9	123.26	478.95	0.029
351	0.5	0.3	0.032					35D	1348.6	114.89	488.55	0.031
352	0.9	0.3	0.030					36D	1350.0	104.37	494.45	0.031
354	0.2	0.4	0.032					37D	1350.9	93.15	507.16	0.032
355	0.4	0.4	0.032					38D	1351.9	81.63	515.29	0.031
356	0.5	0.4	0.031					39D	1353.3	68.97	521.19	0.029
357	0.7	0.4	0.029					40D	1355.5	55.02	520.43	0.033
361	0.9	0.5	0.032					41D	1356.8	42.84	512.69	0.029
363	0.1	0.6	0.030					42D	1360.9	115.72	428.92	0.016
364	0.2	0.6	0.030					43D	1360.7	124.34	441.15	0.023
365	0.4	0.6	0.032					44D	1359.7	130.58	452.74	0.032
366	0.6	0.6	0.032					45D	1359.5	133.66	466.33	0.033
367	0.7	0.6	0.028					46D	1359.8	128.57	479.54	0.031
368	0.9	0.6	0.030					47D	1360.0	119.66	489.71	0.029
371	0.9	0.7	0.029					48D	1361.1	109.53	499.35	0.026
373	0.1	0.8	0.029					49D	1362.4	98.70	508.42	0.027
374	0.4	0.8	0.031					50D	1363.8	6.87	516.36	0.029

TABLE 3. Continued

ONS Pod					ONS Pod					Upper Fuselage				
T/C	XO, in.	YO, in.	ZO, in.	b, in.	T/C	XO, in.	YO, in.	ZO, in.	b, in.	T/C	X/L	PHI, deg	b, in.	
51D	1365.3	74.61	524.20	0.030	76D	1386.9	104.23	511.85	0.025	182	0.4	180	0.026	
52D	1367.4	60.48	524.50	0.034	77D	1398.2	140.63	456.75	0.034	183	0.45	180	0.026	
53D	1369.0	48.26	518.62	0.030	78D	1395.7	142.72	471.17	0.040	185	0.55	180	0.026	
54D	1370.3	36.90	508.92	0.027	79D	1395.4	137.55	483.60	0.035	186	0.60	180	0.025	
55D	1373.1	120.67	431.05	0.019	80D	1407.8	143.07	458.22	0.035	187	0.65	180	0.024	
56D	1372.1	128.48	442.97	0.024	81D	1408.2	144.85	472.53	0.040	188	0.70	180	0.025	
57D	1371.2	134.78	454.73	0.033	82D	1408.3	138.82	486.10	0.035	189	0.75	180	0.0255	
58D	1371.1	137.31	467.72	0.037	83D	1420.5	115.46	403.82	0.035	223	0.40	157.5	0.034	
59D	1372.0	132.02	481.22	0.034	84D	1420.3	146.41	474.10	0.040	224	0.45	157.5	0.034	
60D	1372.9	122.88	491.72	0.032	85D	1420.7	140.53	487.50	0.034	225	0.50	157.5	0.034	
61D	1373.7	112.41	501.33	0.029	86D	1433.1	147.19	461.84	0.034	226	0.55	157.5	0.035	
62D	1375.3	100.96	510.88	0.026	87D	1432.7	147.95	474.98	0.038	227	0.60	157.5	0.034	
63D	1376.4	89.49	519.21	0.024	88D	1433.3	142.34	488.33	0.031	228	0.65	157.5	0.0325	
64D	1378.0	77.00	525.93	0.032	89D	1486.4	115.78	421.03	0.027	230	0.75	157.5	0.03	
65D	1379.7	63.26	527.07	0.036	90D	1494.5	123.25	431.10	0.029	231	0.80	157.5	0.032	
67D	1382.4	38.65	512.32	0.027	91D	1502.7	115.78	421.03	0.025	234	0.40	135.0	0.03	
68D	1385.9	115.78	421.02	0.020						235	0.45	135.0	0.03	
69D	1385.6	123.25	431.09	0.020						236	0.50	135.0	0.036	
70D	1383.9	131.73	443.72	0.025						237	0.55	135	0.035	
71D	1383.9	137.99	455.55	0.031						238	0.6	135	0.031	
72D	1383.3	140.31	469.43	0.036						239	0.65	135	0.032	
73D	1385.3	134.47	482.98	0.033						240	0.7	135	0.03	
74D	1384.2	125.46	493.31	0.031						241	0.75	135	0.032	
75D	1385.5	114.84	503.23	0.026						242	0.8	135	0.032	
										388	0.4	114	0.031	
										389	0.45	114	0.033	

Upper Fuselage					Forward Fuselage Side				
T/C	X/L	PHI, deg	b, in.		T/C	X/L	ZO, in.	b, in.	
390	0.5	114	0.036		205	0.05	378.4	0.033	
391	0.55	114	0.035		210	0.10	410.0	0.037	
392	0.6	114	0.034		206	0.076	350	0.035	
394	0.7	114	0.034						
395	0.75	114	0.036						
T/C	X/L	Y, in.	b, in.						
124A	0.397	1.128	0.031						
125A	0.396	8.68	0.029						
129A	0.406	1.584	0.034						
410A	0.695	1.572	0.033						
155A	0.790	1.572	0.031						
156A	0.790	0.868	0.026						
157A	0.819	1.582	0.031						
158A	0.819	1.218	0.025						
159A	0.819	0.868	0.028						
160A	0.819	0.308	0.031						
36A	0.817	0.014	0.028						

TABLE 3. Concluded

Forward Fuselage Side				Lower Centerline				Lower Wing				Upper Wing			
T/C	X/L	Y, in.	b, in.	T/C	X/L	PHI, deg	b, in.	T/C	X/C	2Y/B	b, in.	T/C	X/C	2Y/B	b, in.
207	0.10	0.086	0.038	38C	0.930	0	0.027	116C	0.4	0.6	0.032	246	0.05	0.40	0.024
88A	0.247	1.101	0.056	39C	0.975	0	0.023	117C	0.5	0.6	0.032	248	0.40	0.40	0.024
89A	0.248	0.672	0.031	40	1.015	0	0.030	118C	0.6	0.6	0.032	251	0.80	0.40	0.029
102A	0.296	1.638	0.023	42	1.045	0	0.028	129C	0.5	0.7	0.036	249A	0.30	-	0.030
103A	0.256	2.067	0.015	Lower Wing				130C	0.4	0.7	0.035	250	0.75	0.40	0.020
70A	0.199	1.681	0.030	T/C	X/L	YO, in.	b, in.	107	0.9	0.5	0.029	252	0.95	0.40	0.025
45A	0.099	1.041	0.028	50C	0.5	46.8	0.028	120	0.8	0.6	0.030	253	0.025	0.6	0.009
46A	0.099	--	0.030	51C	0.6	46.8	0.025	121	0.85	0.6	0.0305	466	0.07	0.75	0.027
47A	0.099	1.23	0.031	52C	0.7	46.8	0.030	122	0.9	0.6	0.030	467	0.66	0.78	0.024
107A	0.400	0.780	0.024	53C	0.8	46.8	0.030	123	0.95	0.6	0.030	468	0.65	0.80	0.024
Lower Centerline				54C	0.9	46.8	0.028	138	0.3	0.75	0.035	469	0.64	0.83	0.024
T/C	X/L	PHI, deg	b, in.	56C	0.975	46.8	0.028	143	0.9	0.75	0.0305	473	0.45	0.98	0.020
2	0.005	0	0.032	58	1.030	46.8	0.030	144	0.95	0.75	0.030	476	0.60	0.70	0.030
4	0.020	0	0.040	60	1.06	46.8	0.031	147	0.4	0.80	0.031	478	0.10	0.80	0.031
7	0.050	0	0.033	62C	0.5	93.6	0.031	148	0.9	0.80	0.0305	479	0.30	0.80	0.032
12	0.10	0	0.037	64C	0.7	93.6	0.029	153	0.1	0.90	0.030	480	0.40	0.80	0.032
16	0.150	0	0.036	T/C	X/C	2Y/B	b, in.	158	0.8	0.90	0.029	481	0.50	0.80	0.032
21	0.200	0	0.035	75C	0.1	0.3	0.026	159	0.9	0.90	0.028	482	0.73	0.80	0.025
26	0.400	0	0.034	80C	0.6	0.3	0.030	163	0.2	0.95	0.032				
27C	0.450	0	0.033	83	0.5	0.3	0.030	165	0.5	0.95	0.030				
29C	0.550	0	0.030	84	0.95	0.3	0.031	167	0.8	0.95	0.030				
30C	0.600	0	0.030	87C	0.05	0.4	0.031	168	0.9	0.95	0.030				
32C	0.700	0	0.029	96	0.9	0.4	0.026								
34C	0.800	0	0.030	113C	0.1	0.6	0.031								
36C	0.900	0	0.031	114C	0.2	0.6	0.031								

TABLE 4. 56-0 Model Thermocouple Coordinates

Fuselage Side				Fuselage Side				Fuselage Side				Fuselage Side			
T/C	X/L	ZO, in.	b, in.	T/C	X/L	ZO, in.	b, in.	T/C	X/L	ZO, in.	b, in.	T/C	X/L	ZO, in.	b, in.
1	.275	437.5	.0215	26	.670	420.0	.0205	51	.850	400.0	.0130	76	.850	355	.0188
2	.300	442.0	.0210	27	.705	420.0	.0207	52	.875	400.0	.0130	77	.875	355	.0170
3	.325	445.0	.0217	28	.750	420.0	.0203	53	.900	400.0	.0160	78	.900	355	.0172
4	.350	445.0	.0215	29	.800	420.0	.0202	54	.925	400.0	.0170	79	.925	355	.0180
5	.375	445.0	.0212	30	.824	420.0	.0160	55	.950	400.0	.0220	80	.950	355	.0190
6	.400	445.0	.0217	31	.200	400.0	.0210	56	.300	372.5	.0170				
7	.425	445.0	.0215	32	.225	400.0	.0199	57	.325	372.5	.0170				
8	.450	445.0	.0218	33	.250	400.0	.0199	58	.350	372.5	.0170				
9	.475	445.0	.0219	34	.275	400.0	.0186	59	.375	372.5	.0170				
10	.500	445.0	.0220	35	.300	400.0	.0180	60	.400	372.5	.0170				
11	.525	445.0	.0220	36	.325	400.0	.0190	61	.425	372.5	.0170				
12	.550	445.0	.0222	37	.350	400.0	.0192	62	.450	372.5	.0172				
13	.600	445.0	.0220	38	.375	400.0	.0190	63	.475	372.5	.0175				
14	.650	445.0	.0220	39	.400	400.0	.0139	64	.500	372.5	.0180				
15	.700	445.0	.0228	40	.425	400.0	.0188	65	.525	372.5	.0180				
16	.750	445.0	.0220	41	.450	400.0	.0195	66	.550	372.5	.0190				
17	.800	445.0	.0230	42	.475	400.0	.0200	67	.600	372.5	.0193				
18	.285	420.0	.0190	43	.500	400.0	.0200	68	.650	372.5	.0190				
19	.337	420.0	.0189	44	.525	400.0	.0190	69	.700	327.2	.0200				
20	.390	420.0	.0189	45	.550	400.0	.0200	70	.750	372.5	.0200				
21	.426	420.0	.0190	46	.600	400.0	.0205	71	.200	355	.0195				
22	.478	420.0	.020	47	.650	400.0	.0210	72	.225	355	.0190				
23	.530	420.0	.020	48	.700	400.0	.0202	73	.250	355	.0190				
24	.567	420.0	.0205	49	.750	400.0	.0205	74	.275	355	.0180				
25	.620	420.0	.0205	50	.800	400.0	.0208	75	.800	355	.0185				



TABLE 5. 83-0 Model Thermocouple Coordinates

Canopy					
T/C	RH	LINE	YQ, in	b, in.	
177	1.0	4.0	0.0	.030	
178	1.0	6.0	0.0	.044	
179	2.0	6.0	0.0	.047	
180	3.0	3.0	14.0	.029	
181	3.0	4.0	15.0	.030	
182	3.0	5.0	17.0	.032	
183	4.0	1.0	0.0	.028	
184	4.0	2.0	0.0	.031	
185	4.0	3.0	22.0	.027	
186	4.0	4.0	22.0	.028	
187	4.0	5.0	22.0	.030	
188	4.0	6.0	0.0	.059	
189	5.0	3.0	30.0	.032	
190	5.0	4.0	30.0	.032	
191	5.0	5.0	29.0	.034	
192	6.0	2.0	0.0	.032	
193	6.0	6.0	0.0	.043	
194	7.0	3.0	41.0	.029	
195	7.0	4.0	41.0	.028	
196	7.0	5.0	40.0	.029	
197	8.0	1.0	0.0	.022	
198	8.0	2.0	0.0	.026	
199	8.0	3.0	51.0	.030	
200	8.0	4.0	47.0	.032	
201	8.0	5.0	44.0	.032	

Canopy					
T/C	RAY	LINE	YQ, in.	b, in.	
202	8.0	6.0	0.0	.028	
203	9.0	3.0	62.0	.028	
204	9.0	4.0	56.0	.035	
205	9.0	5.0	49.0	.035	
206	10.0	2.0	0.0	.030	
207	10.0	6.0	0.0	.030	
208	11.0	3.0	71.0	.030	
209	11.0	4.0	64.0	.031	
211	12.0	1.0	0.0	.028	
212	12.0	2.0	0.0	.030	
213	12.0	3.0	70.0	.030	
215	12.0	5.0	0.0	.032	
216	12.0	6.0	0.0	.032	
217	12.0	7.0	0.0	.032	
218	13.0	3.0	69.0	.031	
219	13.0	4.0	65.0	.032	
220	13.0	5.0	62.0	.031	
222	14.0	2.0	0.0	.028	
223	14.0	6.0	0.0	.030	

Canopy					
T/C	X/L	ZO, in	b, in.		
224	.197	435.0	.023		
225	.197	490.0	.027		
226	.197	485.0	.024		
227	.197	490.0	.033		
228	.193	485.0	.029		
229	.197	490.0	.029		
230	.242	--	.031		
231	.251	--	.032		
233	.261	572.0	.034		
234	.242	547.5	.031		
235	.251	559.5	.031		
236	.257	567.0	.033		

Cargo Bay Hinges					
T/C	XO, in.	ZO, in.	b, in.		
251	689.8	405.0	.024		
253	737.3	420.0	.033		
254	737.3	415.0	.034		
255	737.3	--	.034		
256	737.3	--	.034		
258	737.3	405.0	.031		
260	783.5	--	.032		
261	783.5	--	.033		
264	783.5	--	.030		
265	783.5	--	.030		
266	850.6	--	.032		
267	850.6	--	.032		
268	850.6	--	.032		
269	850.6	--	.032		
270	850.6	--	.032		
271	850.6	--	.029		
272	850.6	--	.029		

Cargo Bay Hinges					
T/C	XO, in.	ZO, in.	b, in.		
238	602.3	420.0	.030		
239	602.3	420.0	.030		
243	602.3	405.0	.027		
244	602.3	405.0	.026		
245	669.8	420.0	.032		
246	669.8	420.0	.032		
247	669.8	415.0	.033		
248	669.8	415.0	.033		
249	669.8	415.0	.033		
250	669.8	405.0	.028		

Lower Fuselage					
T/C	X/L	PHL, in.	b, in.		
426	.025	350	.021		
427	.025	343	.022		
428	.025	335	.024		
429	.025	324	.026		
430	.025	320	.028		
432	.025	303	.029		

TABLE 5. Continued

Lower Fuselage				Lower Fuselage				Upper Fuselage				Upper Fuselage			
T/C	X/L	PHI, deg	b, in.	T/C	X/L	PHI, deg	b, in.	T/C	X/L	PHI, deg	b, in.	T/C	X/L	PHI, deg	b, in.
280	.023		.021	461	.20	317.	.027	379	.061	180	.028	414	.205	180	.030
434	.025	287.5	.029	462	.20	313.5	.027	380	.065		.023	415	.225		.022
435	.025	280	.029	463	.20	310.5	.026	381	.068		.029	416	.25		.026
436	.025	273	.030	464	.20	307	.025	383	.076		.030	417	.275		.033
437	.051	352.5	.025	465	.20	305	.026	384	.077		.031	418	.300		.035
438	.05	347	.026	466	.20	303	.027	386	.079		.027	419	.325		.033
439	.05	339	.025	467	.20	300.5	.027	387	.102		.028	420	.350		.032
440	.05	334	.024	468	.20	298	.025	388	.116		.021	422	.400		.033
441	.05	327.5	.024	469	.20	295	.028	389	.119		.033	423	.425		.032
442	.05	321.5	.028	470	.20	292	.023	391	.127		.036	421	.375		.033
443	.05	318	.028	471	.20	290	.023	392	.131		.038	425	.475		.034
445	.05	306	.025	472	.20	287	.021	395	.141		.034	Upper RCS Nozzles			
446	.05	300	.025	473	.20	284	.028	398	.152		.032	T/C	X/L	YO, in.	b, in.
447	.05	295	.023	474	.20	278	.023	399	.156		.030	161	.062	-7.5	.027
448	.05	289	.028	475	.20	275.5	.023	400	.158		.030	162	.071		.021
449	.05	284	.026	476	.20	273	.024	401	.161		.029	163	.081		.028
452	.20	351	.023					403	.166		.027	164	.094		.029
453	.20	346	.023	Upper Fuselage				404	.169		.027	165	.098		.028
454	.20	342	.023	T/C	X/L	PHI, deg	b, in.	406	.175		.027	166	.101		.029
455	.20	338	.023	367	.0	180	.026	407	.177		.0289	167	.062	-15.0	.030
456	.20	333	.023	368	.001		.028	408	.180		.033	168	.071		.034
457	.20	330	.023	369	.002		.026	410	.186		.032	169	.081		.027
458	.20	326	.024	371	.006		.022	411	.189		.037	170	.094		.028
459	.20	322	.026	373	.012		.029	412	.193		.031	171	.098		.027
460	.20	320	.026	376	.022		.030	413	.197		.030	172	.101		.029
				378	.028		.026								

TABLE 5. Concluded

Upper RCS Nozzle				Fuselage Right Side				Fuselage Right Side				Fuselage Right Side			
T/C	X/L	YO, in.	b, in.	T/C	X/L	ZO, in.	b, in.	T/C	X/L	ZO, in.	b, in.	T/C	X/L	b, in.	
173	.081	-22.5	.030	324	.225	378	.027	273	.001	0	.029	361	.35	.031	
174	.094	-22.5	.026	325	-	-	.028	274	.0018	0	.029	362	.375	.030	
175	.098	-22.5	.032	326	.275	378	.026	275	.004	0	.031	363	.40	.032	
176	.101	-22.5	.031	327	.300	378	.029	277	.010	0	.029	364	.425	.032	
Fuselage Right Side				328	.325	378	.025	281	.026	0	.029	Lower Centerline			
T/C	X/L	ZO, in.	b, in.	334	.225	400	.026	282	.0299	0	.029	T/C	X/L	PHI, deg	
296	.025	-	.029	335	.250	400	.029	283	.034	0	.030	273	.001		
297	.05	-	.027	336	.275	400	.026	285	.0414	0	.029	274	.0018		
298	.075	-	.027	337	.300	400	.031	286	.0452	0	.031	275	.004		
299	.10	-	.028	338	.325	400	.027	288	.10	0	.029	277	.010		
307	.325	-	.025	344	.325	425	.031	281	.026	0	.029	281	.026		
301	.15	-	.028	345	.350	425	.030	282	.0299	0	.029	282	.0299		
302	.175	-	.031	346	.375	425	.030	283	.034	0	.030	283	.034		
303	.20	-	.028	347	.400	425	.030	285	.0414	0	.029	285	.0414		
304	.225	-	.021	349	-	425	.031	286	.0452	0	.027	286	.0452		
305	.250	-	.028	351	.05	-	.027	288	.10	0	.021	288	.10		
306	.275	-	.034	352	.075	-	.027	289	.15	0	.033	289	.15		
310	-	-	.027	353	.10	-	.026	291	.25	0	.036	291	.25		
311	.200	355	.023	354	.125	-	.027								
312	.225	355	.025	355	.15	-	.027								
313	.250	355	.030	356	.175	-	.031								
314	.275	355	.0279	357	.20	-	.026								
315	.300	355	.031	358	.275	-	.032								
317	.350	355	.031	359	.30	-	.031								
323	.200	378	.026	360	.325	-	.030								







TABLE 7. Photographic Summary

	Camera Type	Frame Rate	Camera Location	View Type*	Roll No.	Run No.	
Schlieren	Camera 1	Varitron 70 mm still	1 per run	Operating side upstream window	Schlieren	722,123 700,739	1-269
	Camera 2	Varitron 70 mm still	1 per run	Operating side downstream window	Schlieren	729,147 774,798	1-269
Oil Flow	Camera 1	Varitron 70 mm still	1 per 2 sec ▲	Top upstream window of 2-port window	View of model bottom surface on centerline	627	77-81
	Camera 2	Varitron 70 mm still	1 per 2 sec ▲	Operating side+ upstream window	View of copilot side of model on centerline	716	262-269
						630	77-81
	Camera 3	Varitron 70 mm still	1 per 2 sec ▲	Tank	View of model top surface on centerline	781	262-269
						687	77-81
	Camera 4	Varitron 70 mm still	1 per 2 sec ▲	Non-operating+ side upstream window	View of pilot side of model on centerline	792	262-269
699						77-81	
					786	262-269	

\* Models were inverted

+ Operating side is on the right looking downstream

▲ Runs 77 and 78 had a frame rate of 1 per sec

# APPENDIX III

## REFERENCE HEAT-TRANSFER COEFFICIENTS

In presenting heat-transfer coefficient results it is convenient to use reference coefficients to normalize the data. Equilibrium stagnation point values derived from the work of Fay and Riddell\* were used to normalize the data obtained in this test. These reference coefficients are given by:

$$H(REF) = \frac{8.17173(PT2)^{1/2}(MUTT)^{0.4} \left[1 - \frac{P}{PT2}\right]^{0.25} [0.2235 + (1.35 \times 10^{-5})(TT+560)]}{(RN)^{1/2}(TT)^{0.15}}$$

and

$$STFR = \frac{H(REF)}{(RHO)(V) [0.2235 + (1.35 \times 10^{-5})(TT + 560)]}$$

where

PT2	Stagnation pressure downstream of a normal shock wave, psia
MUTT	Air viscosity based on TT, lb <sub>f</sub> -sec/ft <sup>2</sup>
P	Free-stream pressure, psia
TT	Tunnel stilling chamber temperature, °R
RN	Reference nose radius, (0.0175 ft or 0.04 ft determined by model scale)
RHO	Free-stream density, lbm/ft <sup>3</sup>
V	Free-stream velocity, ft/sec

\*Fay, J. A. and Riddell, F. R. "Theory of Stagnation Point Heat Transfer in Dissociated Air," Journal of the Aeronautical Sciences, Vol. 25, No. 2, February 1958.



APPENDIX IV

SAMPLE TABULATED DATA

ARVIN/CALSPAN FIELD SERVICES, INC.  
 MEDIC DIVISION  
 WYON KAPPA GAS PNEUMICS FACILITY  
 ARNOLD AIR FORCE STATION, TENNESSEE  
 HASA/HI UNIT HEATING  
 PAGE 1

Run	PURPL	MACH AD	PT,PSIA	YT,DEGR	ALPH	PHI	ALPHA	YAW
172	60-D	7.8N	203.5	1247.7	4.96	0.00	40.04	0.00
T	P	Q	V	W	M	RE	STPM	
DECP	PSIA	FT/SFC	LM/FT3	LM/SEC/FT2	FT-1	(RMS)	(RMS)	
93.01	0.023	1.000	3725.	7.451-04	1.033E+06	2.449E-02	3.969E-07	
DELTA	DELTA	DELTA	DELTA	DELTA	DELTA	DELTA	DELTA	
0.0	0.0	0.0	0.0	0.0	0.0	0.0	0.0	
TC NO	Tm	DT4/UT	QDOT	H(TT)	H(TT)	H(4TT)	H(8TT)	Vertical Tail
	TPC R	DEG/S	RTU/	RTU/FT2-	RTU/FT2-	RTU/FT2-	RTU/FT2-	X/C
			FT2-S	S-DEG R	S-DEG R	S-DEG R	S-DEG R	Z/EV
340	542.2	2.568	0.367	5.204E-04	0.0213	0.372E-04	0.0258	0.1000
341	540.9	0.915	0.131	1.804E-04	0.0075	2.246E-04	0.0092	0.1000
342	540.7	0.732	0.157	1.368E-04	0.0056	1.660E-04	0.0068	0.1000
344	540.6	0.934	0.126	1.767E-04	0.0073	2.170E-04	0.0089	0.1000
345	531.3	0.568	0.080	1.123E-04	0.0046	1.363E-04	0.0056	0.1000
346	DELTA							
347	DELTA							
349	549.0	0.572	0.079	1.119E-04	0.0046	1.358E-04	0.0055	0.1000
350	537.7	0.433	0.060	8.404E-05	0.0035	1.027E-04	0.0042	0.1000
351	536.5	0.350	0.055	7.542E-05	0.0032	9.450E-05	0.0039	0.1000
352	536.6	0.336	0.045	6.373E-05	0.0026	7.730E-05	0.0022	0.1000
354	537.5	0.425	0.060	8.432E-05	0.0034	1.023E-04	0.0042	0.1000
355	DELTA							
356	537.4	0.335	0.046	6.494E-05	0.0027	7.490E-05	0.0032	0.1000
357	537.7	0.343	0.051	7.171E-05	0.0029	8.694E-05	0.0036	0.1000
361	537.7	0.653	0.042	3.707E-04	0.0153	1.573E-04	0.0064	0.1000
363	541.9	1.049	0.218	3.808E-04	0.0126	3.773E-04	0.0153	0.1000
364	540.7	0.785	0.107	1.506E-04	0.0062	1.831E-04	0.0075	0.1000
365	540.0	0.480	0.068	9.067E-05	0.0039	1.174E-04	0.0048	0.1000
366	539.4	0.369	0.052	7.344E-05	0.0030	8.591E-05	0.0038	0.1000
367	539.0	0.113	0.052	7.314E-05	0.0030	8.591E-05	0.0038	0.1000
368	DELTA							
371	DELTA							
373	545.7	2.768	0.367	5.204E-04	0.0213	0.372E-04	0.0258	0.1000
374	540.1	0.693	0.135	1.804E-04	0.0075	2.246E-04	0.0092	0.1000
375	539.6	0.923	0.095	1.361E-04	0.0056	1.660E-04	0.0068	0.1000
376	539.5	0.580	0.070	9.901E-05	0.0046	1.201E-04	0.0064	0.1000
377	540.4	1.504	0.215	3.808E-04	0.0126	3.773E-04	0.0153	0.1000
378	539.4	0.668	0.107	1.506E-04	0.0062	1.831E-04	0.0075	0.1000
379	539.4	0.944	0.126	1.773E-04	0.0073	2.170E-04	0.0089	0.1000
384	539.6	1.303	0.184	2.566E-04	0.0106	3.151E-04	0.0129	0.1000
385	539.0	1.172	0.173	2.494E-04	0.0100	2.967E-04	0.0121	0.1000
386	DELTA							
387	DELTA							
388	DELTA							
389	DELTA							

FILMED

7-8